Instituto Politécnico de Tomar

Escola Superior de Tecnologia de Tomar

Filipe Alexandre Guido Bandeiras

MICROGRID ARCHITECTURE EVALUATION FOR SMALL AND MEDIUM SIZE INDUSTRIES

Dissertação de Mestrado

Mestrado em Engenharia Eletrotécnica
Especialização em Controlo e Eletrónica Industrial

Tomar/Novembro/2017

Instituto Politécnico de Tomar

Escola Superior de Tecnologia de Tomar

Filipe Alexandre Guido Bandeiras

MICROGRID ARCHITECTURE EVALUATION FOR SMALL AND MEDIUM SIZE INDUSTRIES

Dissertação de Mestrado

Orientado por:
Prof. Mário Gomes – IPT/ESTT
Prof. Paulo Coelho – IPT/ESTT

Dissertação apresentada ao Instituto Politécnico de Tomar para o cumprimento dos requisitos necessários à obtenção do grau de Mestre em Engenharia Eletrotécnica – Especialização em Controlo e Eletrónica Industrial

Fundação para a Ciência e a Tecnologia

This work was partially supported by the Portuguese Foundation for Science and Technology (FCT) and by PIDDAC, under the research project INDuGRID – ERANETLAC/0006/2014.

ABSTRACT

Industrial customers are looking for ways to reduce their energy consumption and carbon footprint through energy efficiency measures and clean energy sources such as solar and wind power generation systems. In contrast to large industrial enterprises, it may be difficult for smaller industries to improve their energy efficiency due to limited financial conditions and lack of awareness towards cost-efficient applications of renewable energy sources. Nevertheless, the increased integration of clean energy sources in the industrial sector turned microgrids into an important asset to help mitigate the environmental impact from the use of fossil fuels for power generation. Microgrids contribute to a significant increase in reliability and quality to the supplied power without any disturbances and interruptions. These benefits can only be assured by a protection system capable of operating effectively during any abnormal condition.

This dissertation addresses several aspects aiming to assist in the study of industrial microgrid architectures. This work presents an overview of the most common communication technologies and energy sources for microgrids, as well as control strategies for power converters and other control aspects such as droop control method and hierarchical control. In addition, it also addresses several protection methods that can be implemented in microgrids, including protection devices and earthing schemes commonly adopted in low voltage distribution systems. Finally, a case study is presented in order to observe how a centralized and decentralized deployment of energy sources affects the performance of a small industrial microgrid in different scenarios and fault events.

Keywords: Industrial microgrid, centralized/decentralized architecture, renewable energy sources, energy efficiency, communication technologies, control strategies, protection system, distribution system

RESUMO

Os clientes industriais procuram formas de reduzir o consumo energético e a sua pegada ecológica através de medidas de eficiência energética e fontes de energia limpa, como sistemas de geração de energia solar e eólica. Contrariamente às grandes empresas industriais, pode ser difícil para as pequenas indústrias melhorar a sua eficiência energética devido a condições financeiras limitadas e à falta de consciencialização para as aplicações económicas das fontes de energia renováveis. No entanto, o aumento da integração de fontes de energia limpas no setor industrial fez com que as microrredes se tornassem uma mais valia para atenuar o impacto ambiental associado ao uso de combustíveis fósseis para geração de energia. As microrredes contribuem para um aumento significativo de fiabilidade e qualidade da energia fornecida sem quaisquer distúrbios e interrupções. Estes benefícios só podem ser assegurados com um sistema de proteção que seja capaz de operar efetivamente durante qualquer condição anormal.

Esta dissertação aborda vários aspetos que visam auxiliar no estudo de arquiteturas de microrredes industriais. Este trabalho apresenta uma visão geral das tecnologias de comunicação e fontes de energia mais comuns para microrredes, assim como estratégias de controlo para conversores de potência e outros aspectos de controlo, como o método de droop control e o controlo hierárquico. Além disso, são também abordados vários métodos de proteção que podem ser implementados em microrredes, incluindo dispositivos de proteção e esquemas de ligação à terra frequentemente usados em sistemas de distribuição de baixa tensão. Finalmente, é apresentado um estudo de caso para observar como uma implementação centralizada e descentralizada de fontes de energia afeta o desempenho de uma pequena microrrede industrial em diferentes cenários e eventos de falha.

Palavras-chave: Microrrede industrial, arquitetura centralizada/descentralizada, fontes de energia renováveis, eficiência energética, tecnologias de comunicação, estratégias de controlo, sistema de proteção, sistema de distribuição

ACKNOWLEDGMENTS

First and foremost, I would like to express my sincere gratitude to professor José Fernandes and my advisors Mário Gomes and Paulo Coelho for all the help and guidance with the research and writing of this work. Their continuous support and knowledge were essential throughout the development of the project report that served as baseline to this dissertation and two papers. These papers were later submitted to a conference held in France and granted my first experience as presenter.

Finally, I wish to thank my parents and grandparents for providing me with encouragement throughout my whole life and to my closest friends and colleagues for supporting me during my studies and development of this work.

This work was partially supported by the Portuguese Foundation for Science and Technology (FCT) and by PIDDAC, under the research project INDuGRID – *Efficient energy management in industrial microgrids with high penetration of PV technology*, Ref.: ERANETLAC/0006/2014.

TABLE OF CONTENTS

LIST OF FIGURES

LIST OF TABLES

ACRONYMS AND ABBREVIATIONS

AC	Alternating Current
ADSL	Asymmetric Digital Subscriber Line
AMR	Automatic Meter Reading
ANSI	American National Standards Institute
AON	Active Optical Network
BB-PLC	Broadband Power Line Communication
BS	Battery Storage
CHP	Combined Heat and Power
CPP	Critical-peak Pricing
DC	Direct Current
DER	Distributed Energy Resource
DG	Distributed Generation
DMS	Distribution Management System
DNP	Distributed Network Protocol
DSL	Digital Subscriber Line
DSO	Distribution System Operator
ESCO	Energy Service Company
FC	Fuel Cell
FERC	Federal Regulatory Commission
FW	Flywheel
GHG	Greenhouse Gas

GOOSE	Generic Object Oriented Substation Event
HAWT	Horizontal Axis Wind Turbine
HDSL	High-bit-rate Digital Subscriber Line
HTTP	Hypertext Transfer Protocol
HV	High Voltage
IEC	International Electrotechnical Commission
IED	Intelligent Electronic Device
IP	Internet Protocol
LC	Load Controller
LOS	Line-of-sight
LV	Low Voltage
MC	Microsource Controller
MCFC	Molten Carbonate Fuel Cell
MG	Microgrid
MGCC	Microgrid Central Controller
MH	Micro Hydro
MMS	Manufacturing Message Specification
MPPT	Maximum Power Point Tracking
MT	Micro Turbine
MV	Medium Voltage
NB-PLC	Narrowband Power Line Communication
NLOS	Non-line-of-sight
NTP	Network Timing Protocol
PAFC	Phosphoric Acid Fuel Cell
PCC	Point of Common Coupling

PEMFC	Proton Exchange Membrane Fuel Cell
PEN	Protective Earth Neutral
PHS	Pumped Hydro Storage
PLC	Power Line Communication
PON	Passive Optical Network
PV	Photovoltaic
RES	Renewable Energy Source
RTP	Real-time Pricing
RTU	Remote Terminal Unit
SC	Supercapacitor
SCADA	Supervisory Control and Data Acquisition
SME	Small and Medium-sized Enterprise
SMV	Sampled Measured Values
SOFC	Solid Oxide Fuel Cell
SSH	Secure Shell
STC	Standard Test Conditions
TCP	Transmission Control Protocol
TOU	Time-of-use
UDP	User Datagram Protocol
VAWT	Vertical Axis Wind Turbine
VDSL	Very-high-bit-rate Digital Subscriber Line
VPP	Virtual Power Plant
WLAN	Wireless Local Area Network
WPAN	Wireless Personal Area Network
WT	Wind Turbine

SYMBOLS AND UNITS

A	Ampere
Btu	British Thermal Unit
cm	Centimetre
ºC	Degree Celsius
deg	Degree
E	Power Converter Voltage
F	Frequency
Gbps	Gigabit Per Second
GHz	Gigahertz
I	Current
K	Gain
kbps	Kilobit Per Second
Kg	Kilogram
kHz	Kilohertz
km	Kilometre
k_P	Droop Control Frequency Setting
k_Q	Droop Control Voltage Setting
kV	Kilovolt
kVA	Kilovolt-ampere
kVAr	Kilovolt-ampere Reactive
kW	Kilowatt

kWh	Kilowatt-hour
kWp	Kilowatt-peak
m	Meter
Mbps	Megabit Per Second
MHz	Megahertz
mm	Millimetres
MVA	Megavolt-ampere
MVAr	Megavolt-ampere Reactive
MW	Megawatt
MWh	Megawatt-hour
P	Active Power
pu	Per-unit
Q	Reactive Power
R	Resistance
S	Apparent Power
V	Volt
V	Voltage
W	Watt
Wh	Watt-hour
Wp	Watt-peak
X	Reactance
Z	Impedance
δ	Power Converter Voltage Angle
Δf	Frequency Correction Parameter
ΔV	Voltage Correction Parameter

θ	Voltage Angle
Ω	Ohm

1. INTRODUCTION

During the past decades there has been an important development in power systems as a result of an efficient planning and growth in innovation, which led to a considerable quality improvement to the supplied electricity. Nevertheless, the improved quality of the power system is not yet present in every location. Isolated and remote locations still have a defective and faulty power grid with constant power outages. During a power outage of the public power grid, customers may have to wait for days before being reconnected to the power grid and industries that operate with crucial loads cannot afford any power interruption. A failure in the power supply may lead to significant technical problems, production and financial losses [1]. With the integration of distributed generation (DG) into the grid, the reliability and safety of the electric power system became major concerns across the industry, but it also brought the opportunity to include renewable energy sources (RES) and smart control strategies for crucial load supplying in the event of power outages. The environmental concerns associated with power generation from fossil fuels are encouraging industrial customers to look for an alternative clean energy source. This led to the opportunity of considering renewable solutions, such as solar and wind power generation systems. The photovoltaic (PV) systems went through a fast growth in the last decade and these systems are generally characterized by high installation costs, but low operation costs [2]. In addition, there has been a decrease in the module prices of PV systems and the power generation coincides with the peak energy demand during the day [3]. Such systems are an appropriate option for an efficient, reliable and clean industrial power generation system.

This work consists of several chapters addressing different aspects to assist in the study of industrial microgrids. This first chapter briefly introduced a few concerns about the quality of the supplied energy and power outages in the industrial sector, more specifically in isolated and remote locations. It also addressed the fast growth of clean energy sources in power systems due to environmental concerns and decrease in prices. Chapter 2 presents a brief overview of the industrial sector and small and medium-sized enterprises, as well as their energy consumption and barriers to implement energy efficiency measures, along with the benefits of an efficient energy management and demand response measures in the industry. Chapter 3 introduces the definition of microgrid and how it differs from a conventional passive grid, along with the control architecture and other control aspects such as the droop control method and hierarchical control. Chapter 4 addresses the communication architecture of a microgrid and overviews different communication technologies and protocols that can be implemented in microgrids. Chapter 5 presents a simple architecture of a microgrid to introduce different technologies for generation and storage units, including typical installation costs, efficiency and power rates. Chapter 6 addresses the power converters classification according to their operation in a microgrid, along with an overview of control strategies for power converters. Chapter 7 introduces several microgrid protection strategies and devices adopted to protect feeders, buses and energy resources, as well as an overview of the earthing systems commonly used in low voltage distribution networks. Chapter 8 presents the case study of a small scale industrial microgrid in order to observe how a centralized and decentralized deployment of generation units affects the performance of the microgrid in different scenarios and fault events. Chapter 9 is a conclusion to this work and concludes which architecture configuration is the best fitting for small industrial microgrids, based on aspects addressed in the previous sections.

2. OVERVIEW OF THE INDUSTRIAL SECTOR

The industrial sector has the highest delivered energy consumption rates among all sectors. As reported in [4], this sector consumes around 54% of the total delivered energy in the world. The industrial sector can be categorized into three distinct categories according to the energy intensity of each industry type. Industries can be classified as energy intensive manufacturing, non-energy intensive manufacturing and non-manufacturing.

The manufacturing industries such as pulp and paper, iron and steel, non-metallic minerals, non-ferrous metals, basic chemicals, petroleum refineries, food and beverage are classified as energy intensive industries. Together, these count for about half of all industrial sector energy consumption. Manufacturing industries that include printing, pharmaceutical products, specialty chemicals and consumer chemicals, as well as fabricated metal products, computer, electronic and optical products, electrical equipment and machinery are classified as non-energy intensive industries. All industries that include activities such as agriculture, forestry, fishing, mining and construction are classified as non-manufacturing industries [5]. Industrial sector energy consumption varies by region and country, according to differences in industrial gross output, energy intensity and the composition of industries. Energy intensity is measured as final energy consumed per unit of gross output [4].

2.1. Small and medium-sized enterprises

According to [5], small and medium-sized enterprises (SMEs) can be defined as non-substantial and independent companies that employ less than a certain number of employees. Depending on this number, enterprises can be classified into micro, small and medium sized enterprises. The criteria for defining the size of an enterprise may differ across countries and it is also dependent on the company annual turnover or balance sheet total. The European Commission defines an upper limit of 250 employees and an annual turnover up to 50 million euro or a balance sheet total below 43 million euro for medium-sized enterprises. This limit varies from 20 employees in New Zealand to 1000 employees in China. A SME in Australia has up to 200 employees and the United States considers SMEs up to 500 employees [7]. Table I shows the categories that define SMEs, according to the European Commission.

Table I – European Commission definition of SMEs

Category	Employees	Turnover (€)	Balance sheet total (€)
Micro	1 – 10	< 2 million	< 2 million
Small	11 – 50	< 10 million	< 10 million
Medium	51 – 250	< 50 million	< 43 million

The EU recommendation 2003/361 states that SMEs represent 90% of all the businesses in the European Union. Globally, SMEs represent around 99% of all enterprises and provide around 60% of employment. It is known that energy efficiency improvements are typically more cost-effective in all commercial and industrial SMEs, because most of these enterprises have not yet taken advantage of energy efficiency programs that have already been implemented in the larger sectors. As well as energy cost savings and long run positive earnings, energy efficiency improvements may also help mitigate risks when implemented in SMEs. Due to their limited financial condition, SMEs are more vulnerable to market prices increases than larger scale enterprises. At the same time, most SMEs are sensible to power supply disruptions and outages, given their lack of back-up energy systems and on-site generation. Energy efficiency improvements may help reducing these risks, improve energy quality and increase profitability in SMEs [7]. However, smaller enterprises with limited resources and financial conditions may not be capable of implementing energy efficiency programs. Nonetheless, these energy savings can be achieved simply by adopting no-cost and low-cost measures to help reducing energy waste. In the United Kingdom, it is estimated that 40% of the energy savings implemented in SMEs are achieved with minimal financial investment support [8]. Manufacturing SMEs have the highest energy consumption rates among all SMEs. In the United States, the energy demand of manufacturing SMEs is about 50% of the total energy consumed by industry. In Italy, manufacturing SMEs energy consumption is about 70% of the total industrial energy demand. Energy demand of manufacturing SMEs in China is estimated to be almost 2.5 times more than the energy demand of large manufacturing enterprises [7].

2.2. Efficient energy management

As previously mentioned in section 2.1, it may be difficult for some SMEs to adopt energy efficiency measures in order to reduce their carbon footprint and energy consumption. Smaller enterprises are unaware of energy efficiency improvements and cost-efficient applications of RES. Lack of motivation and information, as well as no qualified personnel and limited financial conditions are the main barriers to implementing energy efficiency measures in SMEs [9]. Moreover, banks often refuse to engage with small enterprises, because of their lack of collateral to provide an alternative repayment and the high transaction cost of small loans [7].

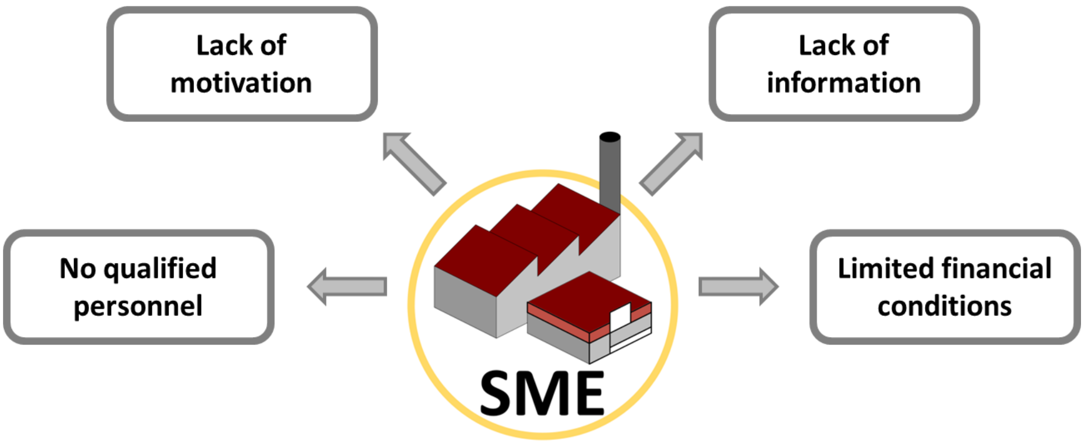

Figure 1 – Main barriers to energy efficiency in SMEs

Energy efficiency improvements in the industrial sector can go from simple no-cost and low-cost measures to large investments such as RES and the integration of smart grids. The no-cost and low-cost measures can be as straightforward as turning off lights and equipment when not in use, fixing sources of energy losses such as leaks or acquiring energy efficient equipment.

An efficient energy management provides an increase in disposable income and improvements in productivity and air quality. It is an effort to reduce the greenhouse gas (GHG) emissions in the industry and combat the climate change, being the largest contribution to GHG abatement with 49% of the savings projected for 2030 [10]. The increased deployment of low-carbon technologies in the industrial sector has been an important asset to mitigate the environmental impact from the use of fossil fuels for power generation. Altogether, the low-carbon technologies account for almost 25% of the primary energy demand projected for 2030, according to the INDC scenario [10]. This rapidly growth of low-carbon technologies is a result of energy policies and incentives implemented towards the use of RES and other low-carbon options.

2.3. Demand response

According to the definition proposed by the Federal Regulatory Commission (FERC), demand response allows customers to intentionally change their energy consumption or load patterns in response to energy prices over time and incentive payments to induce lower energy usage during certain time periods [11]. Demand response is often used to smooth the energy consumption profiles by shifting the load demand between time periods in order to reduce the energy consumption during critical peak periods. Due to this load shifting from demand response measures, potential stresses on the transmission and distribution grid can also be substantially reduced. Industrial customers implement demand response measures to adjust their production processes according to the energy prices, and thus reducing the costs of the energy consumed. Commercial and residential customers often use automated solutions to manage their energy consumption to reduce energy costs. Implementing demand response measures may bring numerous benefits, including economic efficiency, system reliability and environmental benefits associated with the integration of RES [11]. Demand response can be categorized as price-based or incentive-based depending on the encouragement received to implement demand response measures [12].

- **Price-based demand response** denotes a response to changes in energy usage by customers according to changes in the market prices they pay. This type of response includes methods such as real-time pricing (RTP), critical-peak pricing

(CPP) and time-of-use (TOU) pricing. Customers can adjust their energy consumption and load patterns in response to different time periods of electricity prices, reducing their electricity bill by taking advantage of lower price time periods [13].

- **Incentive-based demand response** denotes measures and programs established by the utility that specify a baseline level of energy consumption during certain time periods. These programs provide load reduction incentives for customers, including direct load control, interruptible and curtailable service, demand bidding and buyback programs, emergency demand response programs, capacity market programs and ancillary services market programs. Customers may be penalized if they fail to reduce their energy consumption according to the demand response program they chose to enrol [13].

3. CONCEPT OF MICROGRID

A microgrid (MG) can be seen as an integration of microgeneration, storage units and controllable loads located in a local distribution grid that serves multiple economic, technical and environmental aims. A MG performs an efficient management and coordination of the available resources and it should be capable of handling both normal (grid-connected state) and emergency (islanded state) operation mode [14]. When connected to the main power grid, a MG operates as grid-connected state. In this state, the power converters operate as AC current sources and inject active and reactive power [15]. When disconnected from the main power grid, due to an intentional or unintentional power interruption, a MG operates in islanded mode. In this state, some of the power converters operate as AC voltage sources and regulate the MG voltage [15, 16]. The loads are categorized according to a priority, crucial loads are set to high priority and non-crucial loads are set to low priority. During islanded operation mode, the higher priority loads continue to be supplied in all circumstances and the lower priority loads are sacrificed and can be disconnected when the available energy is low [17].

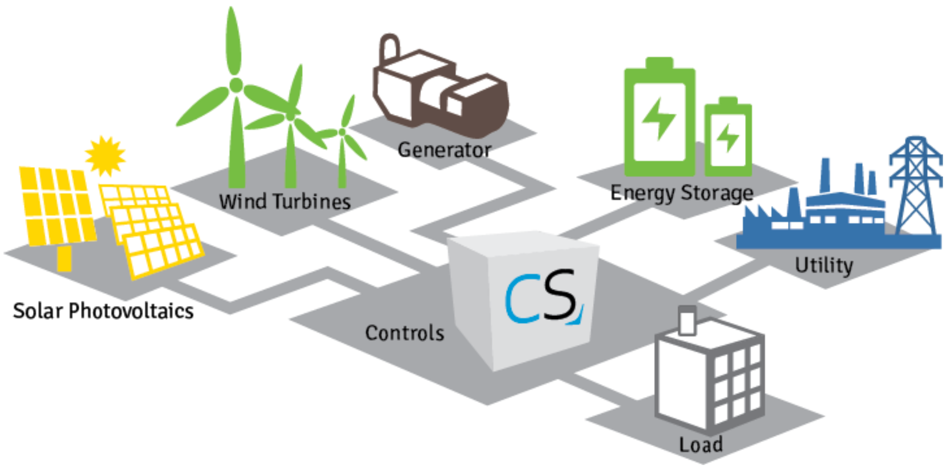

Figure 2 – Concept diagram of a MG [18]

A passive grid with high penetration of distributed microgeneration such as a virtual power plant (VPP) differs from a MG due to the way the grid coordinates and manages the available resources [14]. A MG is more than an aggregator of microgeneration units, storage units and controllable loads that operate collectively with the main public grid or isolated from it. Unlike a conventional passive grid, a MG also purposes a smart and economic solution in order to optimize the energy production and consumption with respect to real time market prices. Furthermore, MGs need an active supervision and control towards the DG and storage units. Table II lists the main differences between a MG and a VPP [14, 19].

Table II – Main differences between MG and VPP

MG	VPP
• Can be disconnected from the public grid and operate autonomously in islanded mode	• Unable to operate without a connection to the public grid
• Requires a set of local energy sources with storage capabilities	• Can integrate resources from a wide geographical area and the absence of energy storage is possible
• Relatively small installed capacity focusing on local consumption	• Much larger scale and installed capacity
• Provides an increase in power quality to the local loads without disturbances and interruptions	• Aims to smooth the integration of a large amount of energy sources into the existing energy systems

A MG includes an electric power grid with distributed energy resources (DER), a communication network and control devices that ensure a safe and optimized grid operation. The DER units, control devices and the communication network may follow different architecture configurations based on how the generation and storage units are deployed along the grid.

3.1. Control architecture

The configuration of the control architecture mainly depends on the existing grid infrastructure. As represented in figure 3, a typical MG hierarchical architecture consists of the distribution management system (DMS), which is responsible for the collaboration between the distribution system operator (DSO), the energy service company (ESCO) and the MG operator; the MG central controller (MGCC), which is responsible for the efficient coordination of the local microsource controllers (MC) and load controllers (LC), provides set points and controls their operation. The MCs are responsible for controlling and monitoring the local distributed generation sources and storage units, while the LCs are responsible for controlling and monitoring the local loads.

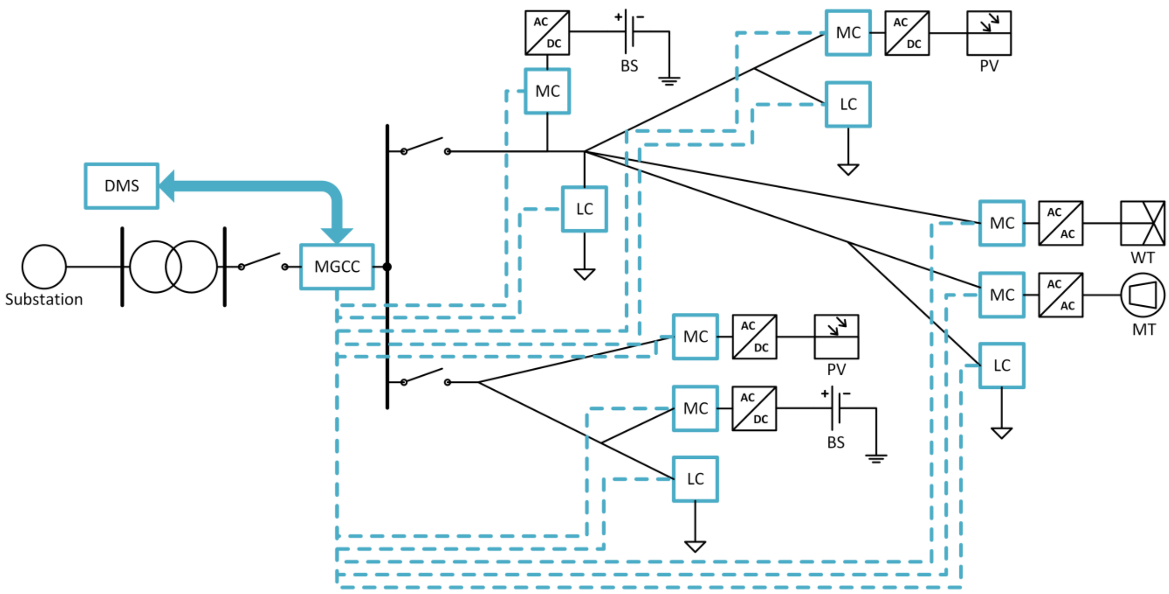

Figure 3 – Control architecture of a MG

The hardware includes the main server and remote terminal units (RTU) or intelligent electronic devices (IED) distributed across the grid that receive data from sensors and send control commands to the DER units, loads and circuit breakers [14].

3.2. Droop control method

The droop control is implemented in the controllers of the power converters and allows voltage and frequency control by regulating the shared active and reactive power according to the reference set point [16]. The main idea is to emulate the operation of a typical synchronous generator, reducing frequency as active power increases and decreasing voltage amplitude as reactive power demand increases [20]. The formulation of the droop equations is based on the active and reactive power shared between a bus with voltage *V* and a power converter with voltage *E* and angle *δ*, as represented in figure 4.

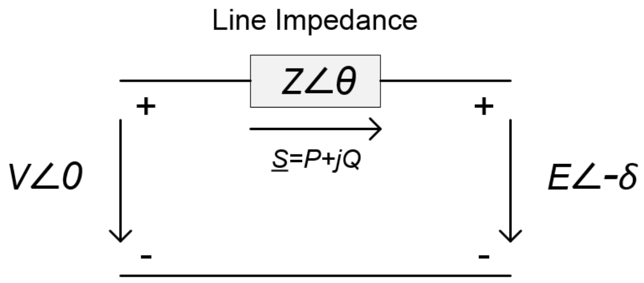

Figure 4 – Power flow in a transmission line

The active power *P* and reactive power *Q* flowing through a transmission line with impedance *Z* and angle θ can be described as [21, 22]:

$$P = \frac{V^2}{Z} \cdot \cos\theta - \frac{V \cdot E}{Z} \cdot \cos(\theta + \delta) \tag{1}$$

$$Q = \frac{V^2}{Z} \cdot \sin\theta - \frac{V \cdot E}{Z} \cdot \sin(\theta + \delta) \tag{2}$$

Defining the line impedance as *Z=R+jX*, results in:

$$P = \frac{V}{X^2+R^2} \cdot (R \cdot V - E \cdot \cos\delta + X \cdot E \cdot \sin\delta)$$

(3)

$$Q = \frac{V}{X^2+R^2} \cdot (X \cdot V - E \cdot \cos\delta - R \cdot E \cdot \sin\delta)$$

(4)

Given that the inductance in typical transmission lines is $X \gg R$, the resistance, *R*, can be neglected:

$$P = \frac{V \cdot E}{X} \cdot \sin\delta$$

(5)

$$Q = \frac{V^2}{X} - \frac{V \cdot E}{X} \cdot \cos\delta$$

(6)

If the power angle δ is small, then $sin\delta=\delta$ and $cos\delta=1$, resulting in the simplified equations:

$$\delta \cong \frac{X \cdot P}{V \cdot E}$$

(7)

$$V - E \cong \frac{X \cdot Q}{V}$$

(8)

The previous equations (7) and (8), show that the power angle depends on the active power, while the voltage difference depends on the reactive power. Frequency is related to the power angle, so by regulating the active and reactive power flow, the voltage and frequency parameters can be determined. Finally, the frequency and voltage control through active and reactive power is given by:

$$f = f_0 - k_P \cdot (P - P_0) \quad (9)$$

$$V = V_0 - k_Q \cdot (Q - Q_0) \quad (10)$$

Where V_0 and f_0 are the nominal voltage and nominal frequency respectively, P_0 and Q_0 are the temporary references for active and reactive power that lead to obtain f_0 and V_0, respectively. k_P and k_Q are the droop control settings for frequency and voltage, respectively. The droop control characteristics plots for frequency and voltage are represented in figure 5.

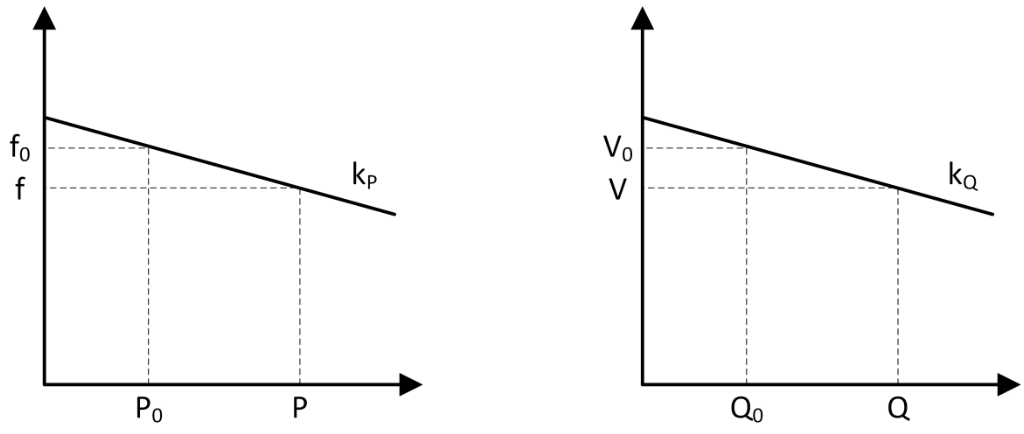

Figure 5 – Frequency and voltage droop control characteristic plots

As represented in figure 5, an increase of active and reactive power will allow frequency and voltage to decrease following a droop control setting. All the parameters are measured and available locally, allowing frequency and voltage regulation according to the injected active and reactive power without the need for a complex communication structure.

3.3. Hierarchical control

A hierarchical control approach consists in three distinct levels of control, as shown in table III. A first layer of control, the primary control level, is responsible for the inner control of the DER units and maintains the voltage and frequency. A second layer, the secondary control level, compensates the voltage and frequency deviations caused by the first level of control. And a third layer, the tertiary control level, manages the power flow between the MG and the main grid according to economic concerns [23].

Table III – Hierarchical control levels

	Implementation	**Control tasks**
Primary	Local	Voltage and frequency maintenance through P/Q droop control
Secondary	Centralized/Decentralized	Synchronization & Voltage and frequency deviations correction
Tertiary	Decentralized	Power flow management & Economically optimal grid operation

3.3.1. Primary control layer

Primary control level provides references to the inner voltage and current control loops of the DER units based on the droop control method and stabilizes the voltage and frequency without a communication between the power converters. The droop control applied to the power converters emulates a synchronous generator, reducing the frequency as active power increases. This principle is implemented in the voltage source converters using the frequency/active power and voltage/reactive power droop control equations.

$$f = f^{*} - k_{P} \cdot (P - P^{*}) \tag{11}$$

$$V = V^{*} - k_{Q} \cdot (Q - Q^{*}) \tag{12}$$

Where f^* and V^* are the reference values for frequency and voltage, respectively. P^* and Q^* are the references set points for the active and the reactive absorbed power.

A virtual impedance loop can also be included in the primary control level to adjust the output impedance of the voltage source converters. The output voltage can be expressed proportionally drooped with respect to the output current.

$$V = V^{*} - Z \cdot I \tag{13}$$

Where V^* is the voltage reference obtained by the conventional droop control equations and Z is the virtual output impedance.

3.3.2. Secondary control layer

Secondary control level ensures that the voltage and frequency deviations are compared with a reference value and regulated towards zero after any variation in power generation and load change. Depending on the MGCC, this control layer can be classified in two main types, centralized and decentralized secondary control. The correction parameters Δf and ΔV are determined using PI compensators.

$$\Delta f = K_{Pf} \cdot (f^{*} - f) + K_{If} \cdot \int (f^{*} - f)\, dt \tag{14}$$

$$\Delta V = K_{PV} \cdot (V^* - V) + K_{IV} \cdot \int (V^* - V)\, dt \tag{15}$$

Where K_{Pf} and K_{PV} are the proportional gains, and K_{If} and K_{IV} are the integral gains for frequency and voltage respectively. The droop control equations are modified with the correction parameters for frequency and voltage, Δf and ΔV.

$$f = f^* - k_P \cdot (P - P^*) + \Delta f \tag{16}$$

$$V = V^* - k_Q \cdot (Q - Q^*) + \Delta V \tag{17}$$

With a centralized secondary control approach, the control is implemented in the MGCC, which interacts and sends references to all the local controllers. In this approach, the voltage and frequency values are measured and compared with the references sent by the MGCC, the resulting deviation value is then sent to the primary control in order to restore the voltage and frequency. With a decentralized secondary approach, the control is implemented locally on all the local controllers. In this approach the values are measured by each local controller and sent to all the other controllers in order to determine an average deviation to restore the voltage and frequency [24].

3.3.3. Tertiary control layer

Tertiary control level takes into account economic aspects based on real time energy prices and manages the power flow between the MG and the main grid. The power flow is controlled by adjusting the voltage and frequency of the DER units aiming for an economically optimal operation for the MG. The grid active and reactive power values are measured and compared with the grid reference values P^{*}_{grid} and Q^{*}_{grid} in order to obtain the frequency and voltage references f^{*} and V^{*}.

$$f^{*} = K_{PP} \cdot \left(P^{*}_{grid} - P_{grid}\right) + K_{IP} \cdot \int \left(P^{*}_{grid} - P_{grid}\right) dt \tag{18}$$

$$V^{*} = \mathrm{K}_{PQ} \cdot \left(Q^{*}_{grid} - Q_{grid}\right) + K_{IQ} \cdot \int \left(Q^{*}_{grid} - Q_{grid}\right) dt \tag{19}$$

Where K_{PP} and K_{PQ} are the proportional gains, and K_{IP} and K_{IQ} are the integral gains for the active and reactive power respectively.

4. COMMUNICATION ARCHITECTURE

In order to monitor and control a system with integrated DER, power converters and variant load patterns, an appropriated communication configuration has to be adopted. The selection of the communication architecture for the MG depends on the existing grid design where the control elements are located, the number of DER units, load clusters locations, data rate, maintenance costs and mainly on the communication technology chosen. The communication architecture can be implemented based on a centralized and decentralized approach. With a centralized architecture (one-to-all), the central controller coordinates the intelligent electronic devices (IED) settings for different operating conditions. With a decentralized architecture (all-to-all), a central controller is discarded and each IED uses the information sent from the other IEDs and coordinates the operation settings. The local controllers are simpler in the centralized approach, since they are not in charge of making decisions. The central controller is responsible of making decisions based on data received from the local controllers. In the decentralized approach, each local controller is in charge of processing data and making decisions, requiring more advanced and complex control devices [14].

The data transmission between the power elements and IEDs and between IEDs and the central controller can mainly follow two physical communication technologies, a wired and a wireless communication technology. A wired communication network does not rely on batteries to operate and generally offers higher speeds. The data transmission rate can easily reach up to 1 Gbps or more in optical cable applications, while a wireless network has a data transmission rate of 600 Mbps (in Wi-Fi networks), slightly less reliable and it is more susceptible to interference. On the other hand, a wireless communication network includes lower installation costs, easier installation of remote terminal units (RTU) and flexibility to add new nodes to the existing network [25, 26]. Depending on the technology adopted, the communication system can also integrate both wired and wireless links in parallel to help reducing data traffic congestions in the wired links and improve the availability of the network [27].

4.1. Wireless communication links

There are several wireless communication technologies that are suitable for MG communication networks, such as Wi-Fi, WiMAX, Cellular 3G/4G, ZigBee and Bluetooth [28, 29]. These technologies may follow distinct IEEE standards and can be distinguished by data transmission rate, operating frequency band and range as presented in table IV.

Table IV – Wireless technologies characteristics [29, 30]

<table>
<tr><th>Family</th><th></th><th>Data rate</th><th>Range</th><th>Frequency</th></tr>
<tr><td rowspan="2">Wi-Fi</td><td>IEEE 802.11e/s</td><td>up to 54 Mbps</td><td rowspan="2">up to 300 m</td><td rowspan="2">2.4 GHz / 5 GHz</td></tr>
<tr><td>IEEE 802.11n</td><td>up to 600 Mbps</td></tr>
<tr><td>WiMAX</td><td>IEEE 802.16</td><td>75 Mbps</td><td>up to 100 km</td><td>2.5 GHz / 3.5 GHz / 5.8 GHz</td></tr>
<tr><td rowspan="2">WPAN</td><td>ZigBee (IEEE 802.15.4)</td><td>20 - 250 kbps</td><td>up to 75 m</td><td>868 MHz / 915 MHz / 2.4 GHz</td></tr>
<tr><td>Bluetooth (IEEE 802.15.1)</td><td>1 - 3 Mbps</td><td>1 - 100 m</td><td>2.4 - 2.485 GHz</td></tr>
<tr><td rowspan="7">Cellular</td><td>GSM</td><td>14.4 kbps</td><td rowspan="2">1 - 10 km</td><td rowspan="2">900 - 1800 MHz</td></tr>
<tr><td>GPRS</td><td>170 kbps</td></tr>
<tr><td>3G</td><td>384 kbps – 2 Mbps</td><td rowspan="2">1 - 10 km</td><td rowspan="3">900 MHz / 2100 MHz
(or 850 MHz / 1900 MHz)</td></tr>
<tr><td>3G (HSPA)</td><td>14.4 Mbps down
5.75 Mbps up</td></tr>
<tr><td>3G (HSPA+)</td><td>84 Mbps down
22 Mbps up</td><td>up to 5 km</td></tr>
<tr><td>4G (LTE)</td><td>326 Mbps down
86 Mbps up</td><td rowspan="2">up to 5 km
5 - 30 km
30 - 100 km</td><td rowspan="2">800 MHz / 1800 MHz / 2600 MHz
(or 700 MHz / 1700 MHz / 1900 MHz)</td></tr>
<tr><td>4G (LTE Advanced)</td><td>1 Gbps down
500 Mbps up</td></tr>
</table>

4.1.1. Wi-Fi

A Wi-Fi network provides a flexible, reliable and high speed local wireless communication based on the IEEE 802.11x standards. Wi-Fi 802.11e and 802.11s standard specifications propose the implementation of the wireless home and local area network (WLAN) on the 2.4 GHz / 5 GHz frequency bands, offering 54 Mbps data transmission speed and range up to 300 m. Wi-Fi 802.11n standard specifications propose implementations on the 2.4 GHz / 5 GHz frequency bands up to 300 m with data rates of 600 Mbps. Because Wi-Fi networks operate on the unlicensed spectrum, their deployment is relatively cheap. But at the same time, the use of a crowded unlicensed spectrum also makes Wi-Fi networks more susceptible to interference [29].

4.1.2. WiMAX

A WiMAX network offers a long coverage area and high speed wireless communication based on the IEEE 802.16x standards. WiMAX 802.16 standard specifications define implementation on the 2.5 GHz / 3.5 GHz / 5.8 GHz frequency bands with data transmission speeds of 75 Mbps. It also proposes a coverage area up to a maximum of 100 kms depending on the performance. Other WiMAX IEEE standards allow implementation on higher frequency bands with lower data rates. However, high spectrum frequencies cannot support non-line-of-sight (NLOS) transmission scenarios, requiring a line-of-sight (LOS) scenario to operate, where a path between the receiver and transmitter is visible. WiMAX provides good performance over long distances and supports thousands of simultaneous users. However, a WiMAX network requires a complex network management [29].

4.1.3. ZigBee

A ZigBee network provides a low power and low cost local wireless communication based on the IEEE 802.15.4 standards. It proposes a worldwide use on the 2.4 GHz frequency band (Europe – 868 MHz and North America – 915 MHz) and a typical range up to 75 m with low data rates of 20-250 kbps. The ZigBee Pro supports an increased coverage area up to 1600 m [30]. ZigBee is considered an ideal network for energy metering and management applications that require both low power consumption and low bandwidth with a low deployment cost [31]. This technology offers a simple and cheap solution, making it the most adopted technology for wireless personal area networks (WPAN) in commercial and industrial applications [29].

4.1.4. Bluetooth

A Bluetooth network provides a low power local wireless communication with low deployment costs based on the IEEE 802.15.1 standards. It operates on the 2.4-2.485 GHz frequency band with a data transmission speed of 1-3 Mbps and a coverage area of 1-100 m. Bluetooth networks offers less latency than ZigBee or Wi-Fi networks and can be often used in local monitoring applications [28, 32]. Due to the limited range, both Bluetooth and ZigBee networks are unable to scale to large networks [29]. This technology suffers from security concerns, but it is still widely adopted for wireless personal area networks (WPAN) with low cost deployment.

4.1.5. Cellular 3G/4G

The 3rd Generation (3G) and 4th Generation (4G) cellular networks provide long distance wireless communications with ranges up to 10 km and 100 km, respectively. Cellular 3G operates on the 900 MHz / 2100 MHz frequency band (or 850 MHz / 1900 MHz) with a coverage area of 1-10 km and data rates of 384 kbps to 2 Mbps. 3G (HSPA) offers data download speeds of 14.4 Mbps and data upload speeds of 5.75 Mbps with ranges up to 10 km. 3G (HSPA+) offers an increased data download speed of 84 Mbps and a data upload speed of 22 Mbps with a lower coverage area up to 5 km. Cellular 4G operates on the 800 MHz / 1800 MHz / 2600 MHz frequency band (or 700 MHz / 1700 MHz / 1900 MHz) with an extended range up to 100 km with a performance hit. The optimum and acceptable operation of cellular 4G is at ranges up to 5 km and 5-30 km, respectively. The operation over longer distances up to 100 km has a reduced performance. 4G (LTE) provides a data download speed of 326 Mbps and a data upload speed of 86 Mbps. 4G (LTE Advanced) offers a much higher data download speed of 1 Gbps and data upload speed of 500 Mbps. The low power consumption of terminal equipment and an extensive data coverage area with high flexibility are the main advantages of cellular networks [29]. Furthermore, public cellular networks are already deployed and can be used with no maintenance costs [28]. However, there are high costs associated with the use of a service provider network and there is no guarantee of service during abnormal weather conditions [31].

4.2. Wired communication links

The MG communication network may also be integrated with physical wired communication links such as PLC, DSL and optical fibre [29, 33]. The wired technologies follow different IEEE and ITU standards and are distinguished by data transmission rate, operating frequency band and range as presented in table V.

Table V – Wired technologies characteristics [29, 30]

Family		Data rate	Range	Frequency
PLC	NB-PLC (ITU-T G.hnem, IEEE 1901.2)	up to 500 kbps	+150 km	3 - 500 kHz
	BB-PLC (ITU-T G.hn, IEEE 1901)	up to 10 Mbps	up to 1.5 km	1.8 - 250 MHz
Optical fibre	AON (IEEE 802.3ah)	100 Mbps	up to 10 km	500 MHz*km
	PON (BPON (ITU-T G.983), GPON (ITU-T G.984), EPON (IEEE 802.3ah))	155 - 2448 Mbps	10 - 60 km	
xDSL	HDSL (ITU G.991.1)	2 Mbps	up to 3.6 km	0.1 - 292 kHz
	ADSL (ITU G.992.1)	8 Mbps down 1.3 Mbps up	up to 4 km	25 kHz – 1.1 MHz
	ADSL2 (ITU G.992.3)	12 Mbps down 3.5 Mbps up	up to 7 km	
	ADSL2+ (ITU G.992.5)	24 Mbps down 3.3 Mbps up		25 kHz – 2.2 MHz
	VDSL (ITU G.993.1)	52 - 85 Mbps down 16 - 85 Mbps up	up to 1.2 km	25 kHz – 12 MHz
	VDSL2 (ITU G.993.1)	up to 200 Mbps	300 m – 1.5 km	

4.2.1. PLC

Power line communications (PLC) makes use of existing power lines for data communication. A PLC network provides a cost-effective solution with a low maintenance requirement, since a single infrastructure is used for both data and power transmission [29]. The narrowband PLC (NB-PLC) is based on the ITU-T G.hnem and IEEE 1901.2

standards that define a data transmission speed up to 500 kbps on the 3-500 KHz frequency band and a coverage area of 150 km or more. The broadband PLC (BB-PLC) is based on the ITU-T G.hn and IEEE 1901 standards that define a higher data transmission speed up to 10 Mbps on the 1.8-250 MHz with a shorter coverage area up to 1.5 km. BB-PLC is also capable of providing data rates up to 200 Mbps in very short distances by operating on higher frequency bands. Because PLC makes use of a single infrastructure for data and power decreasing the cost of installation, this communication technology is the preferred solution for metering data transmission and the simplest to implement in smart grid applications. However, the noisy and harsh nature of the power line channel affects the data transmission and may decrease the quality of signal [31].

4.2.2. Optical fibre

An optical fibre infrastructure provides long distance communication with high data rates with robustness against radio and electromagnetic interferences. However, optical fibre applications are characterized by high installation costs, high terminal equipment costs and difficulty to upgrade. These disadvantages prevent optical fibre communications from being widely adopted in smart grids [29]. Active optical network (AON) is based on the IEEE 802.3ah standard and offers data transmission speeds of 100 Mbps with a range up to 10 km. AON requires electrically powered switching equipment such as routers or a switch aggregator to manage signal distribution and direct signals to the correct destination. Passive optical network (PON) technologies provide higher data transmission speeds of 155-2448 Mbps with ranges from 10 km to 60 km, depending on the standard used. PON does not require electrically powered switching equipment, instead it uses optical splitters to separate and collect the signals. Optical fibre applications operate on the 500 MHz frequency band for distances of 1 km (500 MHz*km).

4.2.3. DSL

Digital subscriber lines (DSL) uses telephone line infrastructures to transmit digital data. This avoids additional communication infrastructures when a telephone line infrastructure is already deployed [29]. High-bit-rate DSL (HDSL) is based on the ITU G.991.1 and supports data transmission rates up to 2 Mbps on the 0.1-292 kHz frequency band and a maximum coverage of 3.6 km. Asymmetric DSL (ADSL) is based on the ITU G.992.1 and provides a data download speed of 8 Mbps and a data upload speed of 1.3 Mbps on the 25 kHz to 1.1 MHz frequency bands with a coverage area up to 4 km. Asymmetric DSL version 2 (ADSL2) is based on the ITU G.992.3 and provides a higher data download speed of 12 Mbps and a higher data upload speed of 3.5 Mbps on the 25 kHz to 1.1 MHz frequency bands with an increased coverage area up to 7 km. Asymmetric DSL version 2 plus (ADSL2+) is based on the ITU G.992.5 and provides increased data download speed of 24 Mbps and a slightly lower data upload speed of 3.3 Mbps on the 25 kHz to 2.2 MHz frequency bands with a coverage area up to 7 km. Very-high-bit-rate DSL (VDSL) is based on the ITU G.993.1 and supports an increased data download speed of 52-85 Mbps and data upload speed of 16-85 Mbps on the 25 kHz to 12 MHz frequency bands with reduced maximum coverage of 1.2 km. Very-high-bit-rate DSL version 2 (VDSL2) supports data transmission speeds up to 200 Mbps with a typical range from 300 m to 1.5 km. In order to use DSL networks, a communication fee must be paid to the telecommunication operator and the network needs to be regularly maintained [29, 31].

4.3. Communication protocols and standards

The Internet protocol suite (TCP/IP) is a set of communication protocols organized into four distinct layers [27]. The application layer is the highest layer and provides protocols that enable process-to-process data communication. Some of the protocols can be Hypertext Transfer Protocol (HTTP), Secure Shell (SSH), Network Timing Protocol (NTP), Distributed Network Protocol (DNP3) and Modbus. The transport layer establishes data channels and provides host-to-host data communication through protocols such as Transmission Control Protocol (TCP) and User Datagram Protocol (UDP). The internet layer provides authentication and defines the addressing and routing structures through internet protocols IPv4 and IPv6. The link layer is the lowest layer and defines methods for the local network communication link. Table VI shows the protocols for each layer of the TCP/IP model.

Table VI – TCP/IP model layers

	Layer	Protocols	Function
1	Application	HTTP, SSH, NTP	Enables process-to-process data communication
2	Transport	TCP, UDP	Provides host-to-host data communication
3	Internet	IPv4, IPv6	Defines the addressing and routing structures
4	Link	Serial, Ethernet	Defines methods for communication link

4.3.1. Modbus

Modbus is a communication protocol that enables communication between a server unit and clients connected to the same network. It is often used in supervisory control and data acquisition (SCADA) systems for a robust communication between supervisory units and remote terminal units (RTU). In a MG with Modbus protocol model, the central controller may act as a server while each IED acts as a client. The data communication between the server and clients is made based on polls from the server. Modbus can be transmitted over RS232, RS485 and Ethernet (TCP/IP) using protocol converters.

4.3.2. DNP3

DNP3 is a new communication protocol often used for data acquisition in SCADA systems that provides a reliable and efficient server to client data communication. Unlike the older protocol Modbus, DNP3 allows client units to be updated without waiting for a poll from the server and supports time synchronization with RTUs by including timestamp variants. DNP3 offers a robust communication and compatibility with a wide range of equipment, being widely used in several industrial applications.

4.3.3. IEC 61850

IEC 61850 is a communication standard that defines data models, events and settings for substation IED configurations. These data models can be mapped to a number of protocols, such as Manufacturing Message Specification (MMS), Generic Object Oriented Substation Event (GOOSE) and Sampled Measured Values (SMV). The IEC 61850 standard enables the integration of protection, control and measurement functions in substation applications.

5. MICROGRID ARCHITECTURE

The implementation of low-carbon energy sources into the power grid is an approach that has been made in order to reduce GHG and carbon emissions in the power sector. This environmental effort led to several MG architecture configurations with high penetration of RES [34].

This section presents a basic architecture of a MG and its DG units, storage units and loads. The main purpose of this architecture is to introduce different technologies for the most common energy resources in MGs. The characteristics for these energy resources are summarized in Appendix A. As represented in figure 6, this architecture consists of a HV/MV transformer substation (T1), MV/LV transformers (T2 and T3), groups of distributed generation (G1 and G2) and load clusters (L1 and L2).

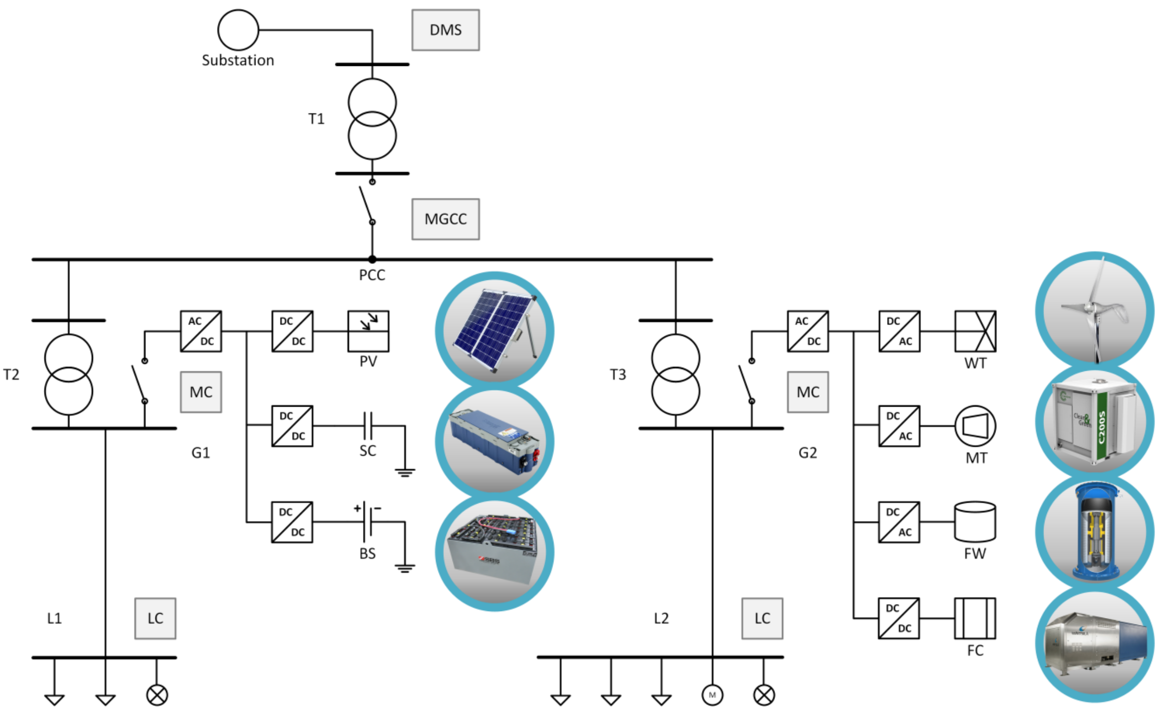

Figure 6 – Basic microgrid architecture

5.1. Distributed generation

Distributed generation (DG) units can include photovoltaic (PV) generation, wind turbines (WT), fuel cells (FC) and micro turbines (MT) [35]. The DG units are located within the same grid and aim to fulfil the local demand. Table VII shows characteristics for the most common DG units adopted in MGs.

Table VII – Distributed generation units [36]

Characteristics	PV	WT	FC	MT
Availability	Location dependent	Location dependent	Any time	Any time
Control	Non-controllable	Non-controllable	Controllable	Controllable
Output power	DC	AC	DC	AC
Conversion	Power electronic converter (DC-DC-AC)	Power electronic converter (AC-DC-AC)	Power electronic converter (DC-DC-AC)	Power electronic converter (AC-DC-AC)
Power flow control	MPPT & DC link voltage control (+P, ±Q)	Turbine speed & DC link voltage control (+P, ±Q)	MPPT & DC link voltage control (+P, ±Q)	Turbine speed & DC link voltage control (+P, ±Q)
GHG emission	None	None	Low	Low

5.1.1. Photovoltaic

A photovoltaic (PV) system converts solar energy into electrical energy by exciting electrons in silicon cells, making this energy source an intermittent RES. The system consists in PV panels that include one or more cell modules and these cells can be wired in parallel to increase current and in series to increase voltage depending on the system requirements.

Major advantages and benefits of a PV system:

- Positive environmental impact;
- Low operation and maintenance costs;
- Long service life;

- Clean and silent operation;
- Generation coincides with peak energy demand.

This solution also brings some disadvantages such as high fixed costs, low cell efficiency, location restrictions and weather dependent. A common way to overcome these disadvantages is to integrate the PV systems with other energy resources.

Solar cells made from crystalline silicon (c-Si) are generally the most common and efficient ones. Depending on the alignment of the silicon molecules and manufacturing process, silicon cells can be made from a single pure crystal of silicon, called monocrystalline (mono-Si) cells and made from an ingot of melted and recrystallized silicon, called polycrystalline (poly-Si) cells. Solar cells can also be made by depositing thin layers of non-crystallized silicon onto a substrate, forming thin-film amorphous (a-Si) cells. Monocrystalline PV panels have the longest service life and also the highest efficiency rates and power output with the least amount of required space. Due to the complicated manufacturing process and purity of the monocrystalline cells, monocrystalline PV panels have the highest production costs and a significant amount of silicon results in waste. Although performance decreases with temperature, monocrystalline technology has a better heat tolerance in warm weather. Polycrystalline PV panels have a slightly lower efficiency and heat tolerance, but the manufacturing process is simpler and costs less, resulting in cheaper panels. Amorphous PV panels are the cheapest to manufacture and can be produced with a flexible substrate, but this technology has the lowest power output and efficiency rates. The typical efficiency rates are around 15% to 23% for monocrystalline PV panels, 13% to 16% for polycrystalline PV panels and 5% to 10% for amorphous PV panels [37]. Table VIII shows the highest confirmed module efficiencies independently measured by a test centre [38].

Table VIII – Solar modules efficiencies [38]

Technology	**Efficiency (%)**	**Area (cm^2)**	**V_{oc} (V)**	**I_{sc} (A)**	**Fill Factor (%)**
Crystalline silicon					
Monocrystalline silicon	24.4 ± 0.5	13177 (da)	79.5	5.04	80.1
Polycrystalline silicon	19.9 ± 0.4	15143 (ap)	78.87	4.795	79.5

Thin-film					
Amorphous silicon	12.3 ± 0.3	14322 (t)	280.1	0.902	69.9

(t) – Total area

(ap) – Aperture area (masked)

(da) – Designated area (masked)

Standard Test Conditions (STC) - Irradiance: 1000 W/m^2; Spectrum: AM 1.5; Temperature: 25°C

Table IX shows the comparison between two solar modules, a monocrystalline module and a polycrystalline module as shown in figures 7a) and 7b). Both solar modules are from Trina Solar, which is one of the top ranked solar panel manufacturers. These PV modules are meant for utility applications and they are equal in size and number of cells.

Table IX – Trina Solar modules comparison [39]

Module	**DUOMAX M+** **Dual glass 72 cell TSM-DEG14 (II)**	**DUOMAX** **Dual glass 72 cell TSM-PEG14**
Solar cells	Monocrystalline (156.75 x 156.75 mm)	Polycrystalline (156.75 x 156.75 mm)
Cell orientation	72 cells (6 x 12)	72 cells (6 x 12)
Peak power range (STC)	335 – 365 Wp	320 – 335 Wp
Maximum power voltage (STC)	37.9 – 39.1 V	37.2 – 37.8 V
Maximum power current (STC)	8.84 – 9.35 A	8.60 – 8.87 A
Module efficiency (STC)	17.1 – 18.6 %	16.3 – 17.1 %

Standard Test Conditions (STC) - Irradiance: 1000 W/m^2; Spectrum: AM 1.5; Temperature: 25°C

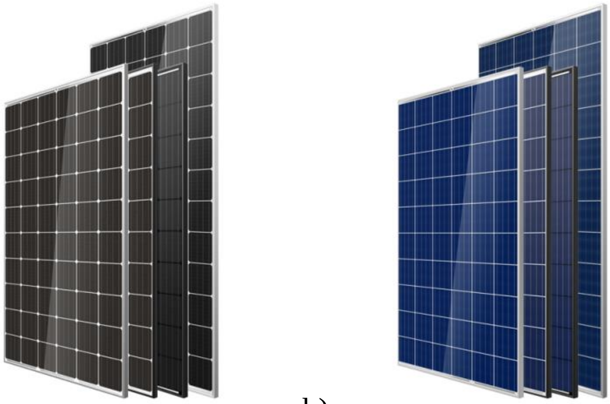

a) b)

Figure 7 – Types of solar cell modules [39]: a) Monocrystalline and b) Polycrystalline

Including solar trackers in PV panels is a common adopted solution to maximize the production of the PV system. Solar tracker devices keep the PV panels oriented towards the sun throughout the day in order to minimize the angle of incidence. The power output is maximized when the angle of incidence is close to 0°, meaning that the light rays have to strike perpendicularly to the PV surface. Solar trackers are categorized as single-axis and dual-axis trackers. Single-axis trackers follow the sun rotating on a single horizontal or vertical axis. The horizontal axis type is used in tropical regions where the position of the sun during noon is usually high. The vertical axis type is generally used in high latitude regions where the position of the sun is not very high. Dual-axis trackers point directly at the sun, moving vertically and horizontally on two axes. The dual-axis solar trackers can be used effectively anywhere in the world [40].

Depending on the geographic location, solar trackers generally offer an increase of 10% to 40% in annual output power over fixed systems [40, 41]. In addition, solar tracker PV systems are able to generate more electricity in the same amount of space needed for stationary PV systems, making tracker units more space efficient than fixed units. However, a solar tracker PV system is more expensive than a stationary PV unit and there is an extra maintenance requirement associated with the additional moving parts. Both stationary and solar tracker PV systems are shown in figures 8a) and 8b).

a)  b) 

Figure 8 – PV systems: a) Fixed [42] and b) Solar tracker [43]

The capital cost estimates of grid-tie DG technologies for residential, commercial and industrial facilities are given in dollars per installed kilowatt of the generating capacity ($/kW). The installed cost of PV systems has been through a substantially decrease due to increased competition in the PV manufacturing industry. According to the cost data provided by the National Renewable Energy Laboratory (NREL), recent installed costs vary from 3000 $/kWp to 4800 $/kWp for PV systems below 10 kWp, between 2500 $/kWp to 4500 $/kWp for 10-100 kWp PV systems and around 1700 $/kWp to 3300 $/kWp for larger 100-1000 kWp PV systems [44].

5.1.2. Wind turbine

A wind turbine (WT) system converts wind energy into electrical energy by using the wind force to turn the blades and make a rotor spin, being also an intermittent RES. The main parts of a WT are the tower, rotor and nacelle. The nacelle contains the brake, gearbox to increase rotational speed (turbines with output power greater than 10 kW) and the generator that is connected to the rotor by the main shaft.

Depending on the rotor orientation, WTs may have vertical axis or horizontal axis configuration as shown in figures 9a) and 9b). Horizontal axis wind turbines (HAWT) have the main rotor shaft, generator and other components on top of a tall tower, the main rotor shaft is arranged horizontally and blades always move perpendicularly to the wind. Vertical axis wind turbines (VAWT) have the generator and main components located near the ground, the main rotor shaft is arranged vertically. Horizontal axis turbines take advantage of the stronger winds due to the tall tower, but it also makes maintenance tasks harder to execute. WTs with horizontal axis configuration require a braking mechanism to prevent the turbine from damaging itself in strong winds and a yaw mechanism to turn the blades towards the wind. Vertical axis turbines take advantage on locations where the wind direction is highly variable, no yaw mechanism required. Unlike the horizontal axis configuration, the vertical axis turbines are located near the ground and only have access to winds with lower speed resulting in a lower output power. Since all the components are placed near the ground, maintenance tasks are simpler and easier than on horizontal axis configuration.

a)

b)

Figure 9 – Types of WT technologies: a) VAWT [45] and b) HAWT [46]

Table X shows the characteristics of small wind turbines for both horizontal and vertical axis configurations.

Table X – Small wind turbine characteristics [44, 47, 48]

Technology	Efficiency	Power	$/kW	Noise	Wind resistance	Starting wind speed
HAWT	20 to 50%	Up to 100 kW	4000 - 8500 (10 - 100 kW)	5 - 60dB	Weak	2.5 - 5 m/s
VAWT	20 to 40%	Up to 100 kW	4000 - 8500 (10 - 100 kW)	0 - 10dB	Strong	1.5 - 3 m/s

5.1.3. Fuel cell

A fuel cell (FC) system converts chemical energy from a fuel into electrical energy through a chemical reaction of positive charged hydrogen ions with an oxidizer such as oxygen. A fuel cell consists of two electrodes and an electrolyte that allows the particles to move between them, the positive electrode is called cathode and the negative is called anode.

The two most common FC technologies for domestic and small scale industrial applications are the proton exchange membrane fuel cells (PEMFC) and solid oxide fuel cells (SOFC). PEMFC operate at low temperatures (80°C) with a polymer electrolyte and use platinum for both electrodes, resulting in higher manufacturing costs. These fuel cells can be used on both portable and stationary applications due to their light weight and compact characteristics. This technology offers fast start capability and rapid response times to load changes. SOFC normally use an yttria-stabilized zirconia (YSZ) electrolyte and operate at high temperatures (around 800°C) enabling any fuel containing hydrogen to be used. Due to the high operating temperature, this technology is well suited for combined heat and power (CHP) applications. Unlike PEMFC, the SOFC are only intended for stationary applications due to their heavy weight and low tolerance for vibrations and frequency stops. Larger scale industrial and commercial applications may use other types of FCs such as molten carbonate fuel cells (MCFC) and phosphoric acid fuel cells (PAFC). MCFC operate at high temperatures (around 650°C) and use a molten carbonate salt suspended in a porous ceramic matrix as the electrolyte. The high temperatures enable non-noble metals to be used as catalysts at the anode and cathode. PAFC use phosphoric acid as the electrolyte and operate at moderate temperatures (around 190°C). Platinum is used as catalyst for the anode and cathode, increasing the system cost. Figure 10 shows a 20 kW SOFC from the Finnish company Wärtsilä.

Figure 10 – 20 kW SOFC from Wärtsilä [49]

The characteristics for each FC technology are listed in table XI.

Table XI – Fuel cell characteristics [50, 51, 52]

Technology	**Efficiency**	**Power**	**$/kW**	**Fuel**	**Operating Temperature**	**CHP**
PEMFC	25 to 35%	Up to 100 kW	1800 - 2000	Hydrogen	~80°C	None
SOFC	50 to 60%	Up to 300 kW	1500 - 1600* 12000 - 15000 (200 - 300 kW)	Natural gas, biogas, other	650 - 1000°C	High
MCFC	43 to 47%	200 kW to 3 MW	1500 - 1600* 12000 - 15000 (200 - 300 kW)	Natural gas, biogas, other	600 - 700°C	High
PAFC	40 to 42%	100 to 400 kW	4000 - 4500	Natural gas	150 - 220°C	Low

* Large scale production

5.1.4. Micro turbine

A micro turbine (MT) system produces heat and electricity from a combustion turbine. The basic components of a MT are the compressor-turbine package mounted on a shaft along with the generator and the recuperator that uses the turbine exhaust heat to preheat the compressed air. The exhaust heat can be recovered by the heat exchanger package and used in CHP applications.

The MTs used for power generation can be single cycle or recuperated micro turbines. In a recuperated turbine, the recovered heat stream from the exhaust is sent back to the incoming air stream in order to boost the temperature of the air stream supplied to the combustor and some of the exhaust heat can be used in CHP applications. Due to preheat, recuperated turbines can save up to around 40% of fuel consumption. In a single cycle turbine, the compressed air is mixed with fuel and burned under constant pressure conditions, resulting hot gas that expands through a turbine. All the exhaust heat can be used in CHP applications, unlikely recuperated turbines that use part of that heat for preheating. Depending on the shaft configuration, MTs can also be classified as single shaft or split shaft micro turbines. In single shaft turbine configurations, all the rotating parts such as compressor, turbine and generator share a common shaft. These turbines usually operate at high speeds (50000 to 120000 rpm) and can be used in applications with constant load changes. In a split shaft turbine configuration, the rotating parts such as compressor and generator are not integrated within the same shaft. The compressor is driven by a compressor turbine and the generator is driven by a power turbine. These turbines operate at lower speeds and offer slower response times to load changes. Figure 11 shows a 200 kW MT module from Capstone.

Figure 11 – 200 kW MT module from Capstone [53]

The characteristics for typical MTs are listed in table XII.

Table XII – Microturbine characteristics [54]

Efficiency	Power	$/kW	Heat rate	CHP
25 to 30% (80% w/ heat recovery)	30 kW to 1 MW	500 - 3000	10000 to 13000 Btu/kWh	High

5.2. Energy storage

Energy storage units can include battery storage (BS), flywheel (FW) systems and even supercapacitors (SC) [35]. The storage elements presented in table XIII are included to ensure an uninterrupted supply of power during outages and to set a power balance after significant load changes. Storage applications can be classified as centralized units and decentralized units. Centralized units are normally installed at transformer substations, this type of storage serves power balance and frequency regulation aims. Decentralized units are normally dispersed over the whole grid, close to loads and generation sources, serving demand response aims.

Table XIII – Storage units [36]

Characteristics	BS	FW	SC
Storage duration	Long-term storage	Short-term storage	Short-term storage
Output power	DC	AC	DC
Conversion	Power electronic converter (DC-DC-AC)	Power electronic converter (AC-DC-AC)	Power electronic converter (DC-DC-AC)
Power flow control	State of charge & voltage/frequency control (+P,±Q)	Speed control (±P,±Q)	State of charge control (±P,±Q)
GHG emission	None	None	None

5.2.1. Battery storage

A battery storage (BS) system stores energy in chemical form and converts the stored chemical energy back to electricity when needed. A battery consists of an electrolyte and two electrodes, the cathode (positive electrode) and anode (negative electrode). In large scale energy storage applications, a group of batteries is joined in parallel for a current increase or in series for voltage increase, forming a battery bank to supply the local loads. Controllers are necessary to prevent the batteries from overcharging.

Most industrial energy storage applications are mainly focused on lithium ion (Li-ion), nickel metal hydride (NiMH) and lead acid (Pb-A) battery technologies. Lithium ion batteries use lithiated metal oxide for the negative electrode and graphitic carbon for the positive electrode, the electrolyte consists of lithium salts in organic carbonates. Generally, these batteries have the best performance, but suffer from safety concerns and high system costs. Lithium is used as electrode material, which is highly reactive, resulting in a high energy density (exceeding 150 Wh/kg) and efficient charging. Nickel metal hydride batteries use metal hydride for the negative electrode and nickel hydroxide for the positive electrode, the alkaline electrolyte often consists of potassium hydroxide. These batteries offer good performance with a relatively safe and durable operation, but with a high system cost and maintenance requirement. Lead acid batteries consist of lead metal and lead dioxide electrodes immersed in sulphuric acid. They have a slow and inefficient charging, but this technology offers a cheap and mature solution. The lead and sulphuric acid contained within the batteries can be a health hazard and cause environmental impacts, which prevent lead acid batteries from being a widely adoption. Figure 12 shows batteries forming a battery bank.

Figure 12 – Battery bank [55]

The characteristics for the most common battery technologies are listed in table XIV.

Table XIV – Battery storage characteristics [56, 57, 58]

Technology	Efficiency	Capacity	Power	Wh/kg	$/kWh	$/kW	Cycles
Li-ion	75 to 90%	Up to 50 MWh	Up to 50 MW	90 - 190	600 - 2500	1200 - 4000	~3000
Pb-A	70 to 90%	Up to 40 MWh	Up to 20 MW	40	200 - 400	300 - 600	500 - 2000
Ni-based	72 to 78%	Up to 20 MWh	Up to 50 MW	50	800 - 1500	500 - 1500	1500 - 3000

5.2.2. Flywheel

A flywheel (FW) system stores mechanical energy in a spinning shaft connected to a generator, the rotor spins building up kinetic energy and converts it to electricity when required. The rotor is suspended by magnetic bearings inside a vacuum enclosure to reduce friction. FWs offer high efficiencies over short timescales and a long service life (over 100000 discharge cycles) with low maintenance and negligible environmental impact. However, these systems suffer from safety concerns due to the high rotor speeds, resulting in severe accidents involving equipment and building damage during the past decades [59]. FW systems are commonly adopted as power quality devices to smooth the transition between power sources and provide a supply of power during short power interruptions. In larger scale, FWs can be used for reactive power support and voltage regulation. These systems are only suitable for high cycling and high power applications with small response times. Figure 13 shows a sectional view of a FW system from Beacon Power.

Figure 13 – Sectional view of a FW system from Beacon Power [60]

Table XV shows the characteristics for FW systems.

Table XV – Flywheel characteristics [57, 58, 61]

Efficiency	Capacity	Power	Wh/kg	W/kg	$/kWh	$/kW	Cycles
85 to 95%	Up to 5 MWh	Up to 20 MW	10 - 30	400 - 1500	1000 - 5000	200 - 600	~100000

5.2.3. Supercapacitors

A supercapacitor (SC) bank stores energy in the form of electric field energy using series of supercapacitors. A SC consists of an electrolyte and two plates (electrodes) separated by a thin insulator. The main advantage is the high power density (around 10 kW/kg), meaning that energy is stored and delivered relatively quickly. Unlikely a battery, SCs cannot store a large amount of energy due to a low energy density, being mostly adopted to help power regulation in intermittent sources and to quickly compensate active and reactive power. SCs also offer a long service life (over 10000 discharge cycles) with high efficiency. A SC storage bank and a single 56V SC module from Maxwell are shown in figures 14a) and 14b).


a)


b)

Figure 14 – 56V SC modules from Maxwell: a) Storage bank [62] and b) Single module [63]

Table XVI shows the typical characteristics for SCs implemented in power regulation and small energy storage applications.

Table XVI – Supercapacitor characteristics [57, 58, 61]

Efficiency	Capacity	Power	Wh/kg	W/kg	$/kWh	$/kW	Cycles
90 to 95%	Up to 1 KWh	Up to 300 KW	5 - 15	10000	300 - 2000	100 - 500	~10000

5.3. Other energy resources

Besides the DG and energy storage units previously mentioned in sections 5.1 and 5.2, there are other energy resources that can be adopted in MGs. In the industrial sector, these energy resources are extremely dependent on the industrial waste products and location. Manufacturing industries are generally located near the raw material source. The pulp industry is usually located near forests to reduce the transportation costs of bulk logs and the paper industry must be located near a river or water reservoirs, because paper manufacturing requires a large amount of water. Taking this into account, micro hydro (MH) systems may be the preferred solution for power generation in river-side applications. A MH system converts the energy of flowing water into electrical energy or mechanical energy. In run-of-river hydro systems, a portion of the river is diverted to a water conveyance (penstock or pipeline) to rotate a turbine that spins a shaft and powers a generator [35]. MH systems can also complement PV systems in many locations, generally because water flow and thus power output, is highest during winter and this is also when the solar energy output is at a minimum. Nevertheless, different regional and seasonal variations must be studied in order to benefit from the complementarity between the two systems [64]. Depending on the terrain topology, pumped hydro storage (PHS) may be considered an option for energy storage. This system allows water to be pumped from a lower reservoir to an upper reservoir during periods of low power demand. When required or during a period of high power demand, water can flow from the upper reservoir to the lower reservoir and through a turbine to generate electricity [58]. The PHS system is usually only applied on large scale energy storage and high power applications, but this system has also shown potential in smaller scale energy storage applications and can be integrated with PV and wind power generation.

Another commonly adopted energy resource in MGs for the industrial sector is cogeneration or combined heat and power (CHP), given that most industrial processes produce waste heat. A CHP system simultaneously generates electricity and useful thermal energy from recovered waste heat. It improves energy efficiency and reduces GHG emissions by reducing the produced waste heat. CHP systems can also be used with sources that operate at high temperatures such as micro turbines and some types of fuel cells. CHP is often seen as an energy efficiency measure rather than an energy resource.

6. POWER CONVERSION

Most of the MG energy sources do not generate power at the grid frequency and cannot be connected directly to the AC grid. These sources need a power converter interface in order to be connected to the grid, unlike synchronous sources such as diesel generators [65]. The power converters integrated with the DG units can be classified in grid-feeding, grid-forming and grid-supporting power converters, depending on their operation [66, 67]. Table XVII shows a brief classification of the different power converter types based on their operation.

Table XVII – Classification of power converters [68]

	Source	Control	Operation
Grid-feeding	Current source	Follows active and reactive power reference values	On-grid operation
Grid-forming	Voltage source	Provides voltage and frequency reference values	Off-grid operation
Grid-supporting	Droop controlled current source	Adjusts active and reactive power references according to voltage and frequency levels	On-grid and off-grid operation
	Droop controlled voltage source	Provides voltage and frequency references according to active and reactive power levels	

Grid-feeding power converters operate as ideal current sources and inject active and reactive power into the grid according to set points often given by a maximum power point tracking (MPPT) algorithm. These power converters are only suitable for grid-connected operation, because they cannot operate during islanded mode if there is no synchronous generator, grid-forming or grid-supporting converter to set the voltage and frequency. Grid-forming power converters operate as ideal AC voltage sources and regulate the grid voltage by setting the amplitude and frequency values. These power converters are suitable for islanded operation mode in order to provide voltage references for grid-feeding power converters. Grid-supporting power converters follow the droop characteristics and act like a synchronous generator, adjusting the voltage and frequency output based on the active and reactive power delivered. These power converters operate as current or voltage sources, suitable for both grid-connected and islanded operation mode.

6.1. Converter control strategies

During grid-connected operation, the power converters inject active and reactive power, following the main grid references. But during islanded mode operation, the power converters are also in charge of supplying the critical loads and regulate the grid voltage. The control of power converters in islanded state may follow two approaches, a master-slave control and a multi-master control approach [69, 70].

6.1.1. Master-slave control

In the master-slave control configuration one converter, acting as master, regulates the voltage and defines the current reference for the other converters based on its own output current. As shown in figure 15, the master converter is associated with an energy storage device and acts as a voltage source, while the slave converters act as current sources. This approach is not suited for systems with dispersed generation, because a higher communication structure and cabling requirement is needed to allow the communication between the master converter and slaves [14]. In this approach, grid outages during islanded operation mode are more likely to occur in the event of voltage source failure, because there is only one voltage source converter regulating the grid voltage.

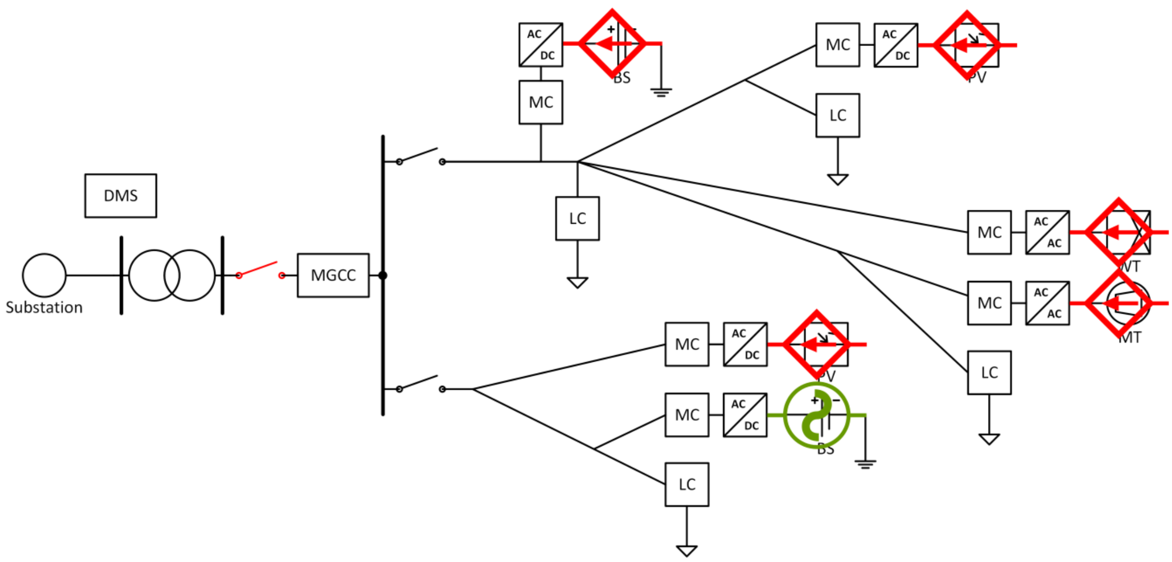

Figure 15 – Master-slave approach (current sources – red and voltage source – green)

6.1.2. Multi-master control

In the multi-master control configuration, all the converters regulate their shared active and reactive power. As shown in figure 16, the two or more master converters operate as voltage sources in parallel, requiring voltage, frequency and phase synchronization between the converters. Synchronization can be met by implementing a droop control and virtual impedance method on the voltage source converters. The parallel configuration of the multiple voltage sources is only possible with output virtual impedance. This control approach is preferred because it eliminates the need for high communication requirement and extra cabling, since the voltage and frequency references are available locally for each converter [14]. In addition, the multi-master approach offers an increase in reliability and in case of a failure event by one of the voltage sources, crucial loads can still be supplied by the remaining voltage sources.

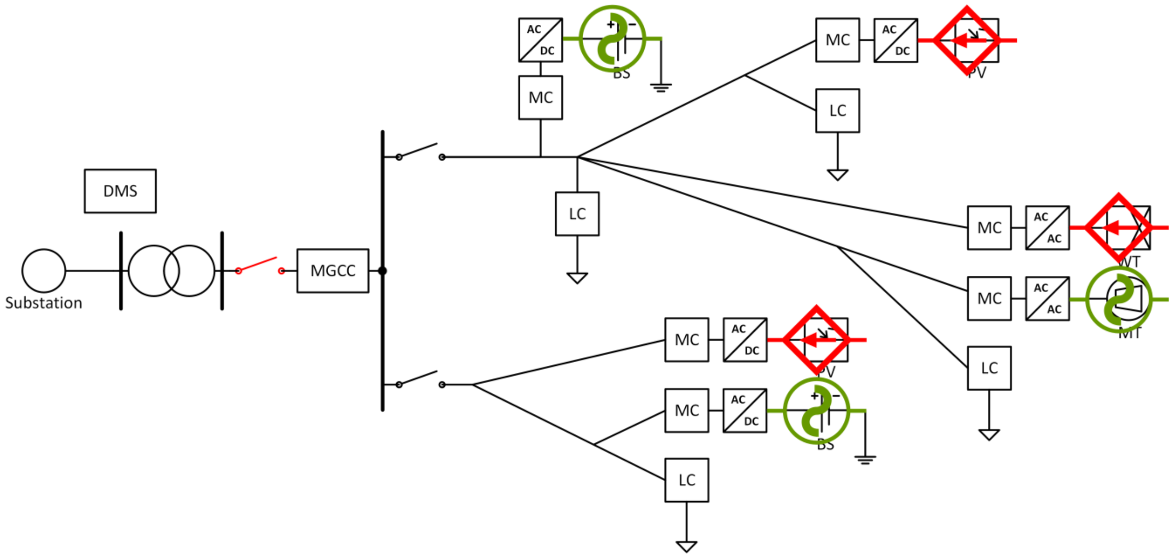

Figure 16 – Multi-master approach (current sources – red and voltage sources – green)

7. MICROGRID PROTECTION

The main requirements for protection systems rely on selectivity, sensitivity and speed. Selectivity aims at disconnecting the minimum grid section possible in order to isolate the fault and maintaining the supply of power to the loads. Sensitivity aims at detecting any abnormal condition exceeding the nominal value. Speed refers to the minimum response time to deal with a fault and avoid further damage to the system. It is also required the maximum possible protection at the lowest cost and the system must be reliable and stable during different operating conditions. In the absence of these protection requirements, problems related to false tripping due to over sensitive protection devices, delayed tripping due to protection devices with a slow response time and faults that remain undetected may arise during certain operating conditions [14]. Due to the integration of DG units with power converter interfaces and the high penetration of synchronous and asynchronous generators, MGs bring several protection issues and challenges. The DG units dispersed along the grid and connected at different locations may cause the power flow in the distribution grid to change from uni-directional to bi-directional if the local power generation exceeds the power demand. In addition, the fault current in a MG is significantly lower during islanded operation mode, because the power converter interfaces associated with the DG units limit the fault current and thus do not supply sufficient current to trigger some of the protection devices. In grid-connected mode, the fault current can be detected by the protection devices, since the public power grid provides an increase in fault current. The high penetration of rotating machines such as synchronous and asynchronous generators into the grid may cause the fault current level to exceed the equipment ratings and cause damage [71]. Moreover, changing fault current levels can be a result of the connection of several DG units with intermittent nature such as photovoltaic (PV) generation systems during islanded operation mode.

The protection system of a MG must be able to quickly react to the public power grid faults and respond to MG failures in order to prevent further damage. The MG transitions between grid-connected and islanded state by means of a static switch that separates the

MG from the public power grid at the point of common coupling (PCC) [72]. When the fault is in the public power grid, the MG protection system must open the static switch and isolate the grid to protect the crucial loads. If the fault is within the MG, the protection system isolates the faulty section from the rest of the grid, allowing the non-faulty sections to continue in operation. Hence, the grid can be segmented into sub-grids and protection sectors according to the location of generation units and loads. The segmentation of a MG into protection zones is achievable in MGs with DER and communication infrastructures that follow a decentralized architecture approach. In a MG with centralized architecture, the grid segmentation into protection zones might not be a viable option due to the inflexible character of the centralized approach during an internal fault in islanded operation mode. Table XVIII lists common protection devices that can be implemented in MGs and their respective ANSI device number [73].

Table XVIII – Protection devices

ANSI number	**Device**
21	Distance relay
25	Synchronism check
27	Under voltage relay
32	Reverse power relay
51	Over current relay
52	Circuit breaker
59	Over voltage relay
67	Directional over current relay
87	Differential relay

A circuit breaker (ANSI 52) is an automatic electrical switch responsible for interrupting the current flow after a fault is detected. Distance relays (ANSI 21) use the fault current and voltage at the relay to determine the impedance between the relay and faulty section of the line. When a fault occurs, the measured impedance is less than the predefined impedance and the relay issues a trip signal to the circuit breaker. Overcurrent relays (ANSI 51) operate when the current exceeds a predefined value and issue a trip signal to the circuit breaker. Directional overcurrent relays (ANSI 67) uses the phase difference between voltage and current to determine the direction to a fault. Reverse power relays (ANSI 32) are directional relays often used in generators to prevent the power from flowing in the reverse direction. When the output of the active generator drops below a predefined value, the relay disconnects the generator to prevent the power from flowing back into the generator. Synchronism check relays (ANSI 25) keep a circuit breaker closed when the measured voltages on both sides are within predefined limits of magnitude, phase angle and frequency. In case of any deviation in frequency between the two sides, the circuit breaker is opened. Overvoltage relays (ANSI 59) operate when the measured voltage exceeds a predefined limit and trigger the circuit breaker to open. Undervoltage relays (ANSI 27) operate when the measured voltage drops below a predefined value. Differential relays (ANSI 87) are used to protect distribution lines, generators and transformers by determining the difference between two or more identical electrical quantities. When a fault occurs, the difference between the input current and output current is not zero and a trip signal is sent to the circuit breakers.

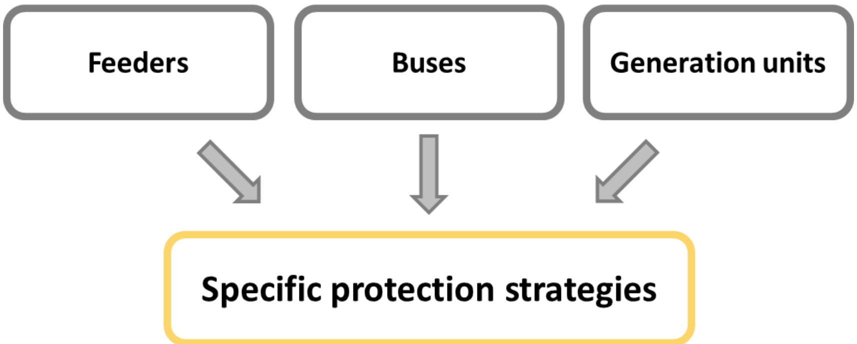

Figure 17 – Requirement for feeders, buses and generation units

Several protection methodologies for MGs are available in the literature. Jenkins et al. in [74] proposed a protection plan using overcurrent relays for grid-connected operation mode. Al-Nasseri et al. in [75] presented a voltage-based protection scheme for islanded operation mode. Then, Dewadasa et al. in [76] proposed a protection scheme using a distance relay that could operate in both grid-connected and islanded modes. Years later, Dewadasa et al. in [77] presented a new approach using differential relays for both grid-connected and islanded operation modes. A comparison between these protection schemes is presented in table XIX.

Table XIX – Comparison between protection schemes [78, 79]

	Operation	Advantages	Disadvantages
Overcurrent (Jenkins et al., 2005)	Grid-connected mode	• Economical solution by using conventional overcurrent relays • No communication link requirement	• Ineffective operation in islanded mode
Voltage (Al-Nasseri et al., 2006)	Islanded mode	• Offers separate protection for DG units	• Cannot operate in grid-connected mode and requires communication links • Ignores high impedance faults
Distance (Dewadasa et al., 2008)	Grid-connected and islanded mode	• Protection zone depends on the line impedance • No communication link requirement	• Unnecessary operation when a load with star-connection is located downstream to the fault
Differential (Dewadasa et al., 2011)	Grid-connected and islanded mode	• Offers feeder, bus and DG unit protection in both grid-connected and islanded mode	• Requires communication links between relays

Groups such as feeders, buses and generation units need specific protection strategies to effectively isolate the detected faults. These groups can be protected using differential relays, as suggested by Dewadasa et al. in [77]. This differential protection strategy can overcome the problem of changing fault current levels caused by the connection of DG units with intermittent nature during islanded operation mode.

7.1. Feeder protection

In normal operation, the current being injected into the feeder is equal to the current leaving the feeder. On the other hand, this condition will not be verified if there is a fault in the feeder. The MG feeders use two protection relays located at the end of the feeder that detect and isolate feeder faults. Differential relays (ANSI 87) are not sensible to bi-directional power flow and change in the number of connections, making these relays preferred for MG feeder protection. The relays contain five elements including three phase elements for each phase to provide high speed protection against high current faults, and two elements for the negative and zero sequence currents to ensure a sensitive protection against lower currents faults. As shown in figure 18, each relay issues a trip signal to the respective local circuit breaker when a fault is detected. The relays at each end of the feeder are connected through a communication link and share synchronized phase current samples [77].

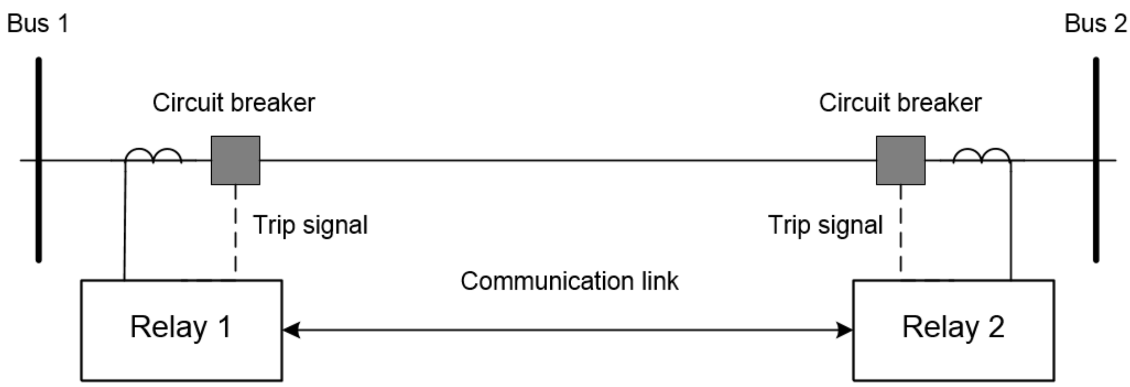

Figure 18 – Differential feeder protection

In a decentralized architecture where the DG units are dispersed along the grid and connected at different locations, the use of a circuit breaker at each end of a feeder can be justified due to bi-directional power flow. However, in case of a centralized architecture where the power flows from the generation group to loads, using a circuit breaker at each end of a feeder increases the cost and might not be economically viable, especially in applications for SMEs. A single circuit breaker feeder configuration can be implemented in branches with uni-directional power flow in order to reduce the cost in both centralized and decentralized grid architectures. The circuit breaker should be deployed at the beginning of the feeder, defined as the side in which the current enters.

7.2. Bus protection

In order to protect the DG units, storage units and loads connected to a bus, protection relays are needed. During a fault, the current injected into a bus node is not equal to the sum of all the currents leaving the bus. Hence, the fault can be detected and isolated using the same protection principle as the feeder differential protection relay [77]. The bus protection operates with the same principle as the differential feeder protection. When a fault is detected in the bus, the relay issues a trip signal to all local circuit breakers in order to isolate the fault, as shown in figure 19.

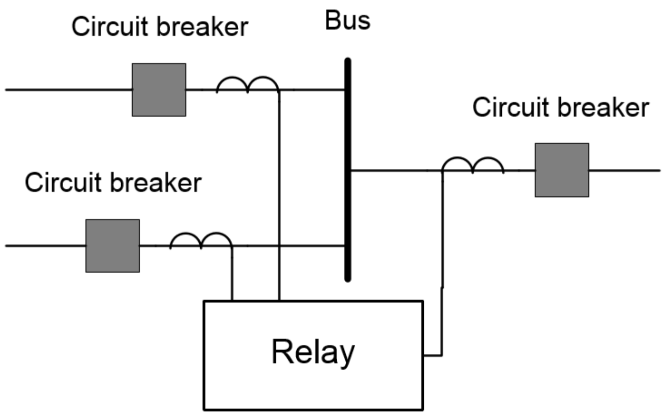

Figure 19 – Differential bus protection

7.3. Distributed generation protection

The DG units are integrated with protection devices such as under voltage relays (ANSI 27), over voltage relays (ANSI 59), reverse power relays (ANSI 32) and synchronism check (ANSI 25). Under voltage and over voltage relays are activated when the voltage is under or over predefined limits and the reverse power relay is activated if the current flows towards the generation unit. A synchronism check device is needed to ensure synchronization and a smooth transition when the generation unit is connected and disconnected from the grid. When a fault is detected, the relay associated with these protection devices will issue a trip signal to the local DG circuit breaker. These protection devices are necessary to ensure the safety of each DG unit and prevent further damage during any abnormal conditions [77].

7.4. Earthing system

The earthing system of LV distribution networks can be categorized in three configurations, TT, IT and TN [80]. These three configurations are defined by five letters, T (direct connection to earth), N (neutral), C (combined), S (separated) and I (isolated from earth). The first letter indicates how the transformer neutral or supply source is earthed and the second letter indicates how the equipment frame is earthed. The third or fourth letters indicate the configuration of the neutral and protective earth conductors and denote their functions [81].

In a TT system, both the transformer neutral and the equipment frames are earthed directly by an earth electrode, as represented in figure 20. It is the most simple and common earthing system, often used in networks containing distributed equipment such as public lighting networks.

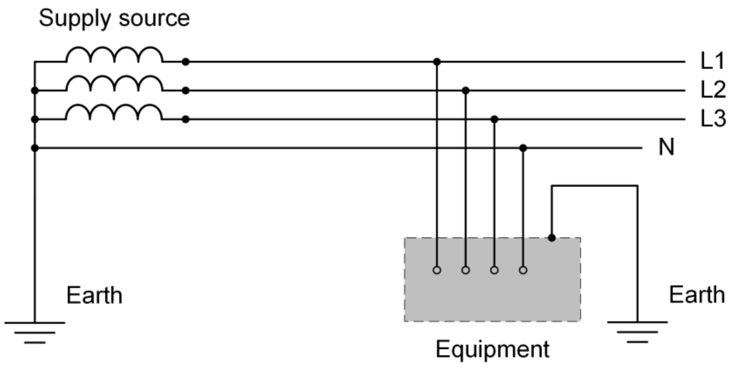

Figure 20 – TT earthing system protection

In an IT system, the transformer neutral is not earthed or not earthed directly and the equipment frames are earthed directly, as represented in figure 21. It is usually used for systems that require high security and reliability.

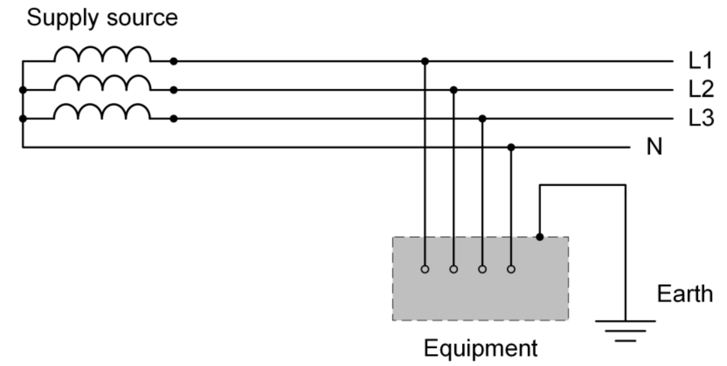

Figure 21 – IT earthing system protection

In a TN system, the transformer neutral is earthed directly and the equipment frames are connected to neutral conductors. TN earthing systems are subdivided in TN-C, TN-S and TN-C-S. TN-C systems combine the neutral conductor (N) and the protective earth conductor (PE) in a single conductor (Protective Earth Neutral, PEN), the same conductor is used for both neutral and protective functions, as represented in figure 22. TN-S systems use different conductors for the neutral and protective functions. As represented in figure 23, the neutral conductor (N) is separated from the protective earth conductor (PE). The TN-C-S system combines both the TN-C and TN-S earthing systems. This system uses a common PEN conductor at the power supply and is then separated in neutral conductor (N) and protective earth conductor (PE) near the loads, as represented in figure 24.

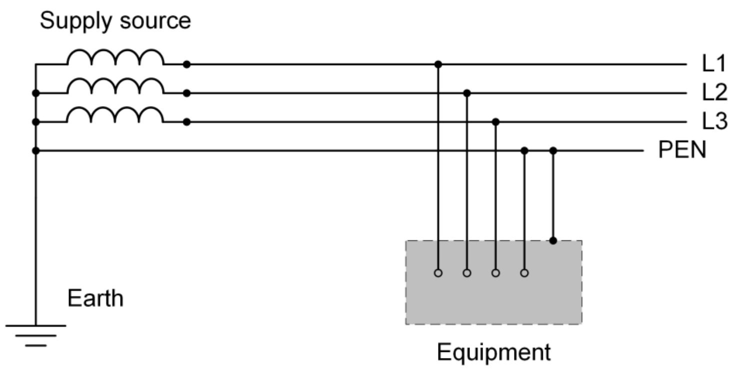

Figure 22 – TN-C earthing system protection

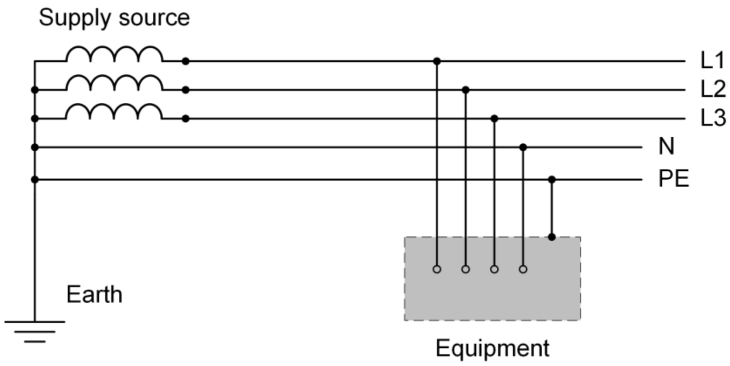

Figure 23 – TN-S earthing system protection

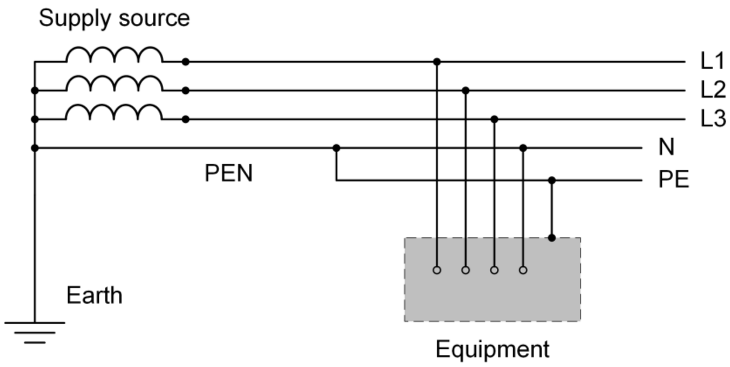

Figure 24 – TN-C-S earthing system protection

IT systems are usually only implemented in private installations or crucial applications such as hospital buildings, while TT and TN systems are widely adopted in public LV distribution networks. For MGs the use of TT and TN earthing systems is suggested as these systems are commonly adopted in LV distribution network applications [80]. TT systems are the most simple to implement and provide flexibility to expand the network. However, there is a possibility of overvoltage stress on the equipment insulation. TN systems work with simple overcurrent protection and provide a low impedance return path for fault currents in the LV grid. In case of an insulation fault, the touch voltages in TN systems are generally smaller than in TT systems due to the low impedance of the PEN conductor and voltage drop in the phase conductor. On the other hand, faults at higher voltage grid levels may migrate into the LV grid.

According to the study presented in [81], the most suitable earthing system for MGs during islanded operation mode is the TN-S. Since the fault current may not be detected in an islanded MG with intermittent DG units, the TN-S system overcomes this problem because the fault current in this system is sufficient enough to trigger the protection devices. Furthermore, protection relays are capable of discriminating between overload current and fault current in a MG with TN-S earthing system implemented.

8. CASE STUDY

This section presents a case study of an industrial MG with centralized and decentralized architecture. The industrial MG developed for this study is based on the transformer, cable, generator and load data presented in [82, 83]. The purpose of this section is to observe how a centralized and decentralized deployment of DERs affects the performance of a small scale industrial MG. The industrial site under study is a small factory that produces paper sheets. It contains a main factory and offices with a nominal power consumption of 320 kW and 80 kW, respectively. There are four step-down transformers inside the MG, transformers T1 and T2 are responsible for decreasing the voltage from 13.8 kV to 480 V, and T3 and T4 decrease the voltage from 480 V to 208 V in order to supply loads such as lights and office equipment. The factory building contains five induction motors, two air conditioning units, an elevator and lights. The office building contains an air conditioning unit, lights and office equipment such as personal computers, printers and fax machines. Figure 25 represents the electrical schematic of the small industrial site under study. The data for each load and transformer is listed in table XX and XXI.

Table XX – Load data

Load	Quantity	Voltage (V)	Unit size (kW)	Power factor	R (Ω)	X (Ω)
Induction motor	5	480	50	0.8	2.946	2.21
Office equipment	4	208	12.5	0.96	1.065	0.307
Air conditioning	3	480	15	0.95	13.844	4.517
Elevator	1	480	30	0.97	7.234	1.804
Light (factory)	5	208	2	0.98	6.92	1.38
Light (offices)	5	208	3	0.98	4.60	0.917

Table XXI – Transformer data

Transformer	Primary (kV)	Secondary (kV)	Load (kW)	Rating (kVA)	R (Ω)	X (Ω)
T1	13.8	0.480	80	200	7.2	29.52
T2	13.8	0.480	320	1000	1.15	8.95
T3	0.480	0.208	65	200	0.0087	0.0357
T4	0.480	0.208	10	40	0.038	0.1440

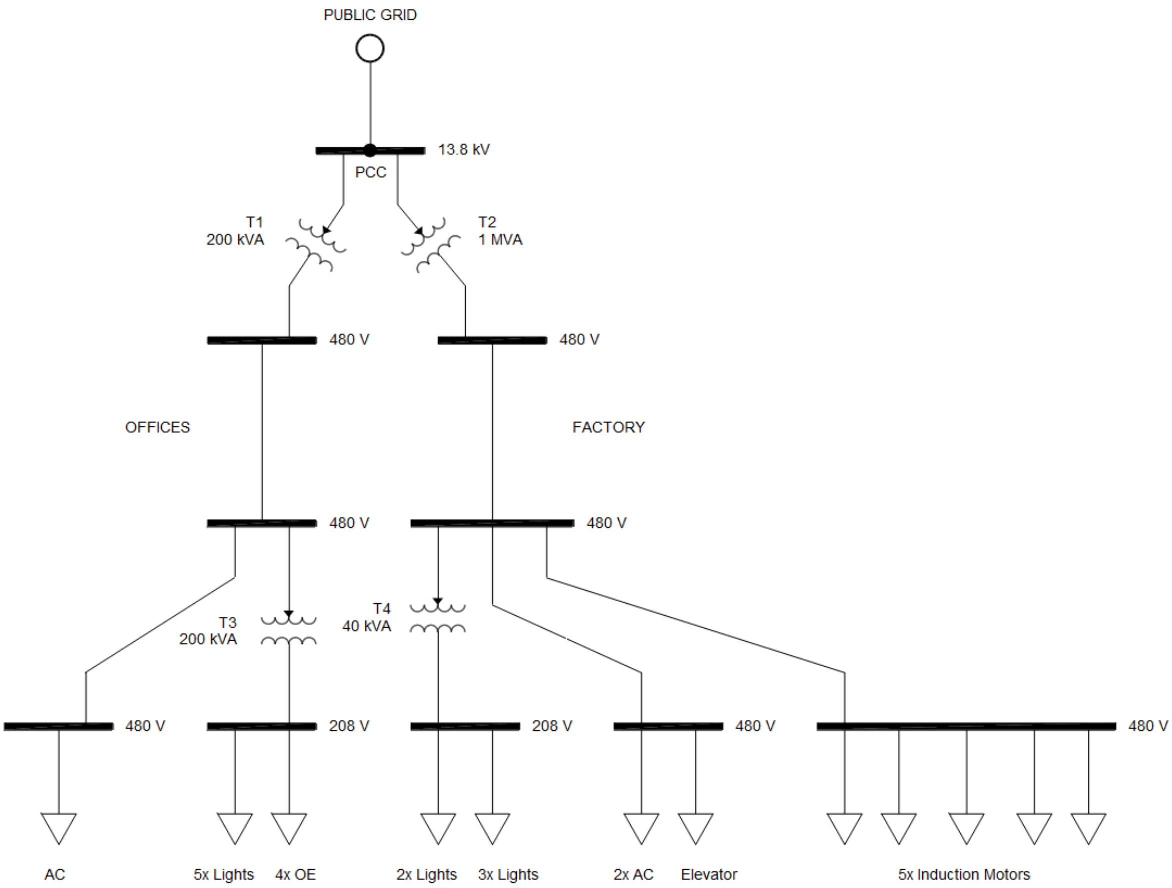

Figure 25 – Electrical schematic of the industrial site

During islanded mode operation, the power generator that simulates the public grid is disconnected from the MG at the PCC. All the loads in the MG follow a priority according to how important they are to the industrial process. Crucial loads are set to high priority and must be supplied in all circumstances in order to avoid jeopardizing the production targets. These loads include the five induction motors with a total power demand of 250 kW located in the factory. The office equipment with a total power demand of 50 kW is set to a medium priority. These loads should be supplied during islanded mode, but they can also be disconnected if the available energy is insufficient to supply them. The remaining loads such as lights, air conditioning units and elevator are set to a low priority. These loads are disconnected from the grid during islanded mode. Both centralized and decentralized MGs will be subjected to the same case scenarios in order to compare their bus voltage and angle profiles obtained from the power flow study using the software PSS/E Xplore.

This initial case is the base scenario and it is equivalent to both centralized and decentralized MG configurations, since all the buses with generation units are disconnected from the MG. In this scenario, the industrial MG is connected to the public grid and both factory and offices are operating at full load (400 kW). All the loads are supplied by the public grid without any power supply from the MG generation units. The public grid must deliver 400 kW in order to supply the loads in the main factory (320 kW) and offices (80 kW). Tables XXII and XXIII show the results obtained from the power flow study for this scenario.

Table XXII – Network generator data

Generator	Bus	PGen (MW)	QGen (MVAr)
Public grid	1	0.4002	0.8855

Table XXIII – Network bus data

Bus	Bus name	Base voltage (kV)	Voltage (pu)	Angle (deg)
1	SWING	13.8	1.0000	0
2	BUS2	0.480	0.9996	-0.0046
3	BUS3	0.480	0.9997	-0.0057
4	BUS4	0.480	0.9996	-0.0013
5	BUS5	0.480	0.9996	-0.0049
6	LOAD1	0.480	0.9996	0.0014

7	LOAD2	0.208	0.9992	-0.0018
8	LOAD3	0.208	0.9992	-0.0038
9	LOAD4	0.480	0.9994	0.0147
10	LOAD5	0.480	0.9995	-0.0045

The voltage obtained for each bus is almost ideal, approximately 1 pu for all buses with the lowest voltage being 0.9992 pu in bus 7 (LOAD2) and bus 8 (LOAD3). This is due to the small grid size and the public grid setting the bus voltage to 1 pu. The results listed in table XXIII show the bus voltage and angle profile for a scenario without power generation from any MG generation units. This initial scenario is compared with the five scenarios for each MG configuration, in the next sections 8.1 and 8.2.

8.1. Centralized MG

A centralized MG architecture for this industrial site is represented in figure 26 and includes a centralized generation group with 360 kW of peak power located at the generation bus, GEN1. This generation group acts as an uninterruptible power generator equipped with a bank of batteries and supplies the crucial loads in the main factory and the office equipment when the available energy is sufficient. The branch data for this configuration is listed in table XXIV.

Table XXIV – Branch data

Branch	**Voltage (kV)**	**Load (kW)**	**Distance (m)**	**R (Ω)**	**X (Ω)**
4 ↔ 2	0.480	360	30	0.002	0.0027
4 ↔ 3	0.480	360	30	0.002	0.0027
2 ↔ 5	0.480	80	30	0.0052	0.0026
5 ↔ 7	0.480	15	10	0.024	0.0015
3 ↔ 6	0.480	320	30	0.002	0.0027
6 ↔ 10	0.480	60	40	0.0392	0.0064

6 ↔ 11	0.480	250	30	0.0023	0.0025

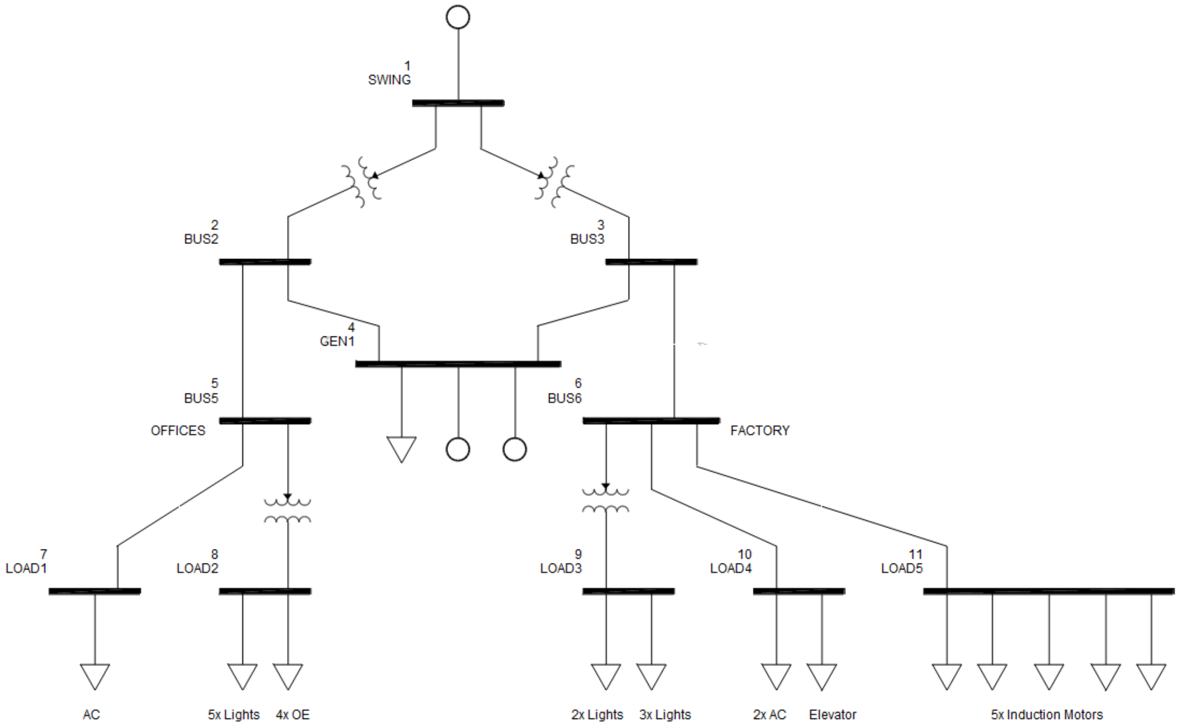

Figure 26 – Schematic of the MG with centralized generation

8.1.1. Case 1C

In this scenario, the MG is connected to the public grid and both factory and offices are operating at full load (400 kW). The loads are supplied by the generation group (GEN1) at peak power generation capacity (360 kW) and the public grid delivers the power needed to supply the remaining loads (40 kW). This represents the most satisfactory scenario during grid-connected operation mode, since the generation group is at its peak power and minimum power is imported from the public grid. Tables XXV and XXVI show the results obtained from the power flow study for this scenario, and the bus voltage and angle profiles are shown in figures 27 and 28.

Table XXV – Network generator data

Generator	Bus	PGen (MW)	QGen (MVAr)
Public grid	1	0.0402	0.1802
GEN1	4	0.3600	0.7049

Table XXVI – Network bus data

Bus	Bus name	Base voltage (kV)	Voltage (pu)	Angle (deg)
1	SWING	13.8	1.0000	0
2	BUS2	0.480	1.0000	0.0001
3	BUS3	0.480	0.9999	-0.0004
4	GEN1	0.480	1.0000	-0.0007
5	BUS5	0.480	0.9999	0.0034
6	BUS6	0.480	0.9998	0.0004
7	LOAD1	0.480	0.9999	0.0060
8	LOAD2	0.208	0.9995	0.0029
9	LOAD3	0.208	0.9995	0.0015
10	LOAD4	0.480	0.9997	0.0200
11	LOAD5	0.480	0.9998	0.0007

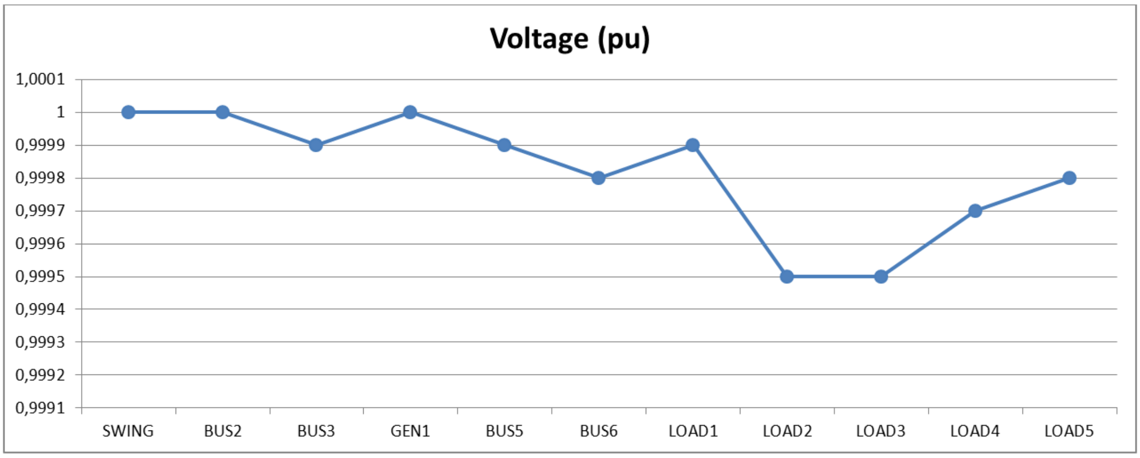

Figure 27 – Bus voltage profile in scenario 1 with centralized generation

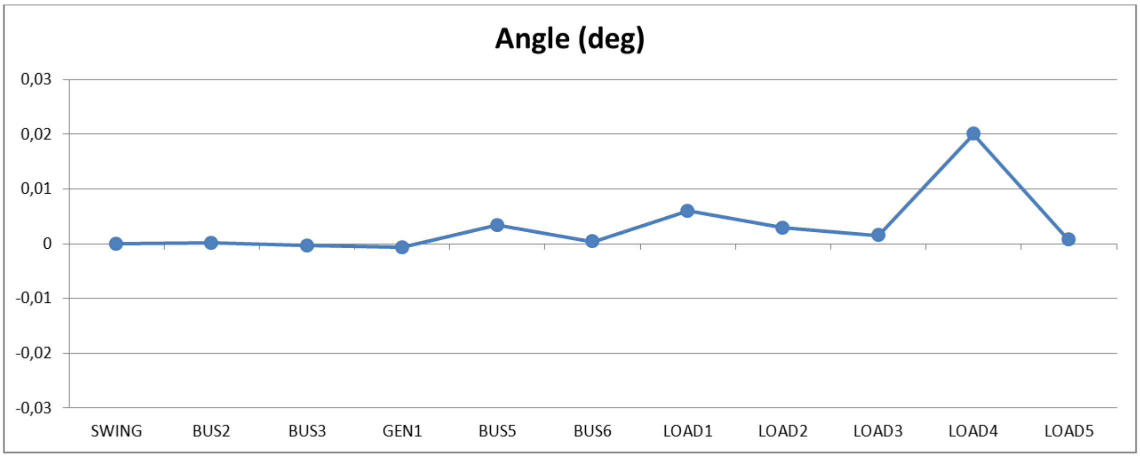

Figure 28 – Bus voltage angle in scenario 1 with centralized generation

When observing the bus voltage profile in figure 27 and bus voltage values listed in table XXVI, it is noticeable a slight improvement over the initial scenario without any MG generation. This is expected, since there is an additional generation group supplying the loads. The lowest bus voltage value is now 0.9995 pu in bus 8 (LOAD2) and bus 9 (LOAD3). As listed in table XXV, the generation group (GEN1) is at peak power delivering 360 kW of active power and 704.9 kVAr of reactive power, while the public grid delivers 40.2 kW and 180.2 kVAr needed to supply the loads and compensate losses.

8.1.2. Case 2C

In this scenario, the MG is connected to the public grid and both factory and offices are operating at full load (400 kW). However, the loads are now supplied by the generation group (GEN1) at 50% of the peak power generation capacity (180 kW). In this less favourable case, the MG needs to import more power from the public grid to supply the loads (220 kW). Tables XXVII and XXVIII show the results obtained from the power flow study for this scenario, and the bus voltage and angle profiles are shown in figures 29 and 30.

Table XXVII – Network generator data

Generator	Bus	PGen (MW)	QGen (MVAr)
Public grid	1	0.2202	0.1339
GEN1	4	0.1800	0.7513

Table XXVIII – Network bus data

Bus	Bus name	Base voltage (kV)	Voltage (pu)	Angle (deg)
1	SWING	13.8	1.0000	0
2	BUS2	0.480	1.0000	-0.0043
3	BUS3	0.480	0.9999	-0.0041
4	GEN1	0.480	1.0000	-0.0055
5	BUS5	0.480	0.9999	-0.0010
6	BUS6	0.480	0.9998	-0.0033
7	LOAD1	0.480	0.9999	0.0016
8	LOAD2	0.208	0.9995	-0.0015
9	LOAD3	0.208	0.9995	-0.0023
10	LOAD4	0.480	0.9997	0.0163
11	LOAD5	0.480	0.9998	-0.0030

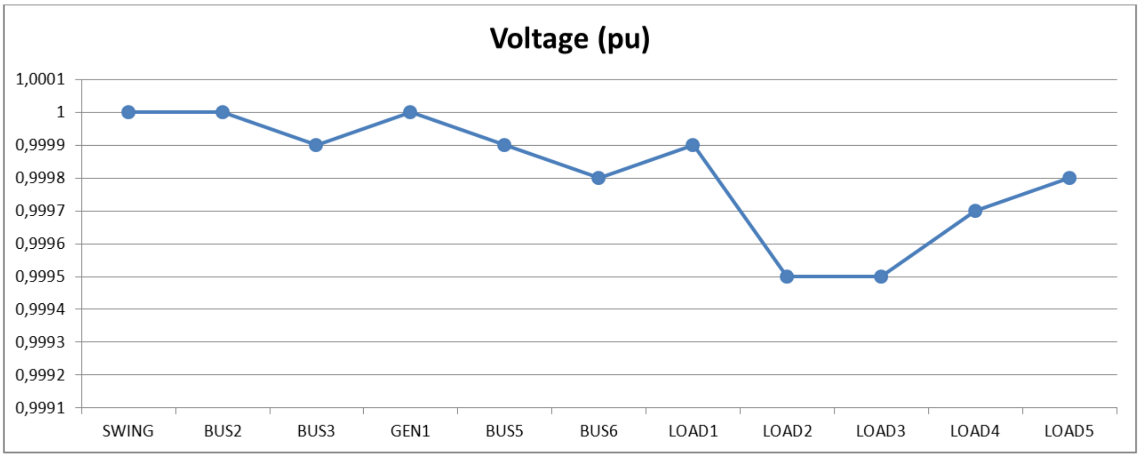

Figure 29 – Bus voltage profile in scenario 2 with centralized generation

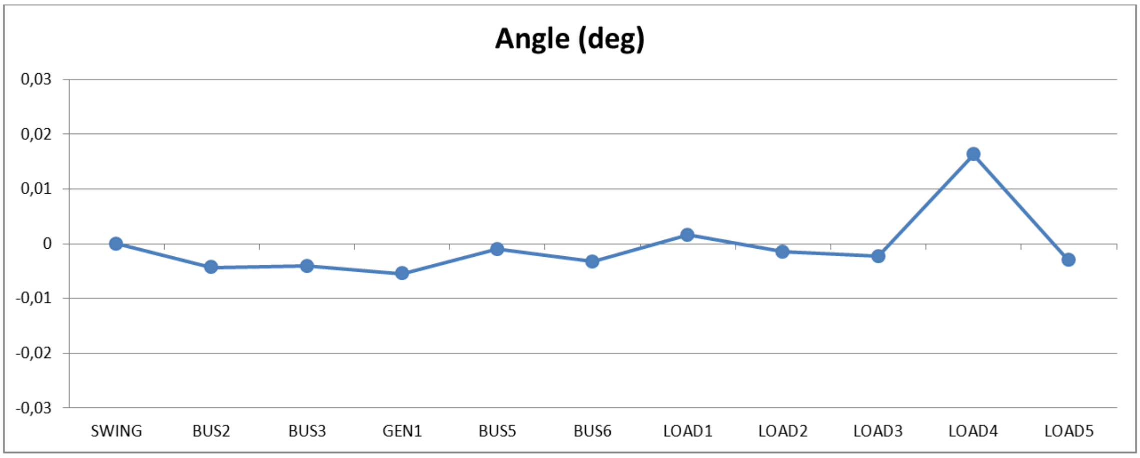

Figure 30 – Bus voltage angle in scenario 2 with centralized generation

When observing the bus voltage profile in figure 29 and bus voltage values listed in table XXVIII, it is also noticeable an improvement over the initial scenario. This is expected, since there is an additional generation group supplying the loads. The lowest bus voltage value is also 0.9995 pu in bus 8 (LOAD2) and bus 9 (LOAD3). As listed in table XXVII, the generation group (GEN1) is at 50% of the peak power generation capacity delivering 180 kW of active power and 751.3 kVAr of reactive power, while the public grid delivers 220.2 kW and 133.9 kVAr needed to supply the loads and compensate losses.

8.1.3. Case 3C

In this scenario, the MG is also connected to the public grid. But the main factory and offices are now operating at 75% (240 kW) and 25% (20 kW), respectively. In the main factory, both air conditioning units and an induction motor are out of service. In the office, most of the lights and office equipment are not in use and the air conditioning unit is also out of service. The loads are supplied by the generation group (GEN1) at 75% of the peak power generation capacity (270 kW). Tables XXIX and XXX show the results obtained from the power flow study for this scenario, and the bus voltage and angle profiles are shown in figures 31 and 32.

Table XXIX – Network generator data

Generator	Bus	PGen (MW)	QGen (MVAr)
Public grid	1	-0.0099	0.1313
GEN1	4	0.2700	0.3777

Table XXX – Network bus data

Bus	Bus name	Base voltage (kV)	Voltage (pu)	Angle (deg)
1	SWING	13.8	1.0000	0
2	BUS2	0.480	1.0000	0.0007
3	BUS3	0.480	0.9999	0.0005
4	GEN1	0.480	1.0000	0.0006
5	BUS5	0.480	1.0000	0.0016
6	BUS6	0.480	0.9999	0.0011
7	LOAD1	0.480	1.0000	0.0016
8	LOAD2	0.208	0.9999	0.0014
9	LOAD3	0.208	0.9995	0.0022
10	LOAD4	0.480	0.9998	0.0123
11	LOAD5	0.480	0.9998	0.0014

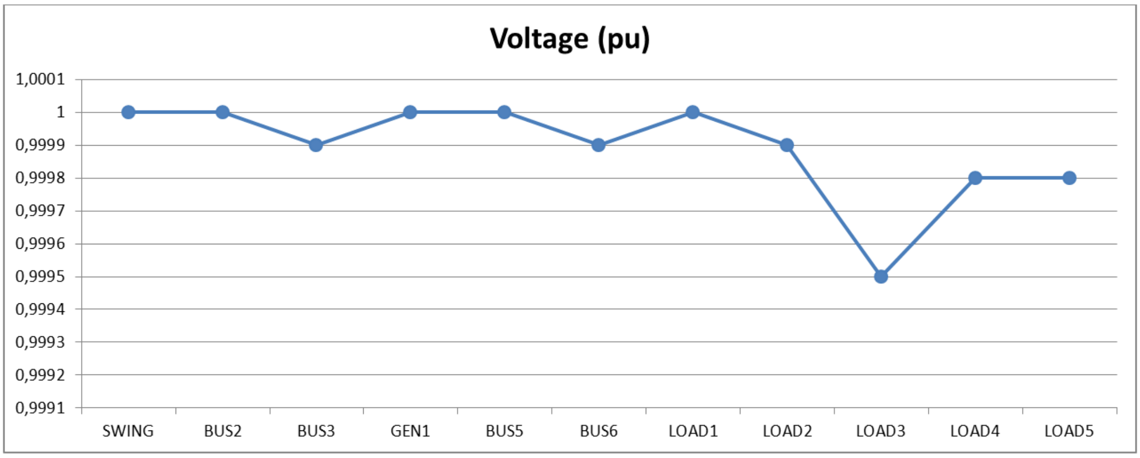

Figure 31 – Bus voltage profile in scenario 3 with centralized generation

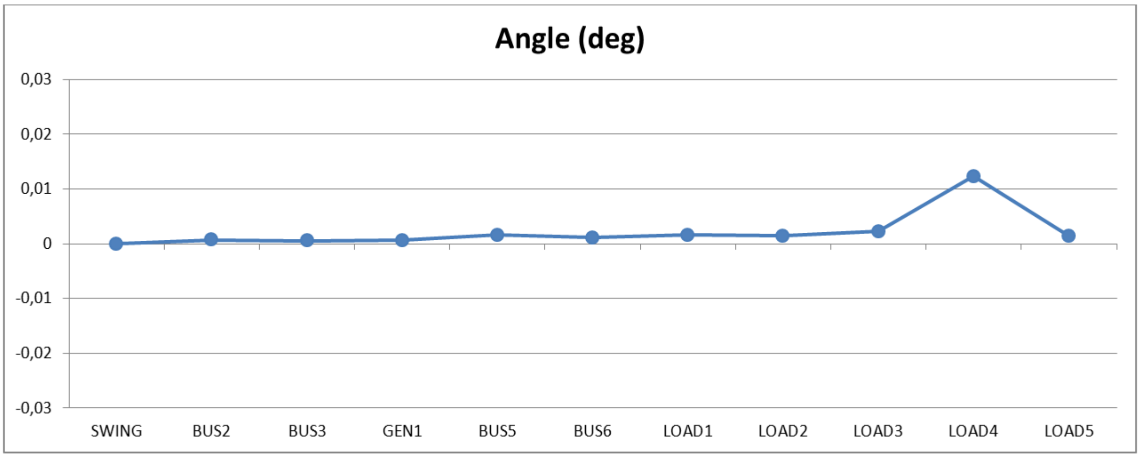

Figure 32 – Bus voltage angle in scenario 3 with centralized generation

When observing the bus voltage profile in figure 31 and bus voltage values listed in table XXX, it is noticeable an improvement over the previous scenarios 1C and 2C, because there was a decrease in power demand to 65% of the total power demand (260 kW). The lowest bus voltage value is 0.9995 pu in bus 9 (LOAD3). As listed in table XXIX, the generation group (GEN1) is at 75% of the peak power generation capacity delivering 270 kW of active power and 377.7 kVAr of reactive power. In this scenario, 9.9 kW of active power is exported to the public grid.

8.1.4. Case 4C

In this scenario, there is no connection to the public grid. MG is operating in islanded mode and all the high and medium priority loads are connected to the grid. The five induction motors with a power demand of 250 kW and the office equipment with a power demand of 50 kW are supplied by the generation group (GEN1) at peak power generation capacity (360 kW). This is the most satisfactory scenario during islanded operation mode, since the generation group is operating at its power peak and the higher priority loads can remain in operation. Tables XXXI and XXXII show the results obtained from the power flow study for this scenario, and the bus voltage and angle profiles are shown in figures 33 and 34.

Table XXXI – Network generator data

Generator	Bus	PGen (MW)	QGen (MVAr)
GEN1	4	0.3001	0.5052

Table XXXII – Network bus data

Bus	Bus name	Base voltage (kV)	Voltage (pu)	Angle (deg)
1	BUS1	13.8	0.9999	0.0001
2	BUS2	0.480	1.0000	0.0005
3	BUS3	0.480	0.9999	-0.00003
4	GEN1*	0.480	1.0000	0
5	BUS5	0.480	0.9999	0.0024
6	BUS6	0.480	0.9999	-0.00004
7	LOAD1	0.480	0.9999	0.0024
8	LOAD2	0.208	0.9997	0.0017
9	LOAD3	0.208	0.9999	-0.00004
10	LOAD4	0.480	0.9999	-0.00004
11	LOAD5	0.480	0.9998	0.0003

* Bus GEN1 is defined as slack bus (swing bus)

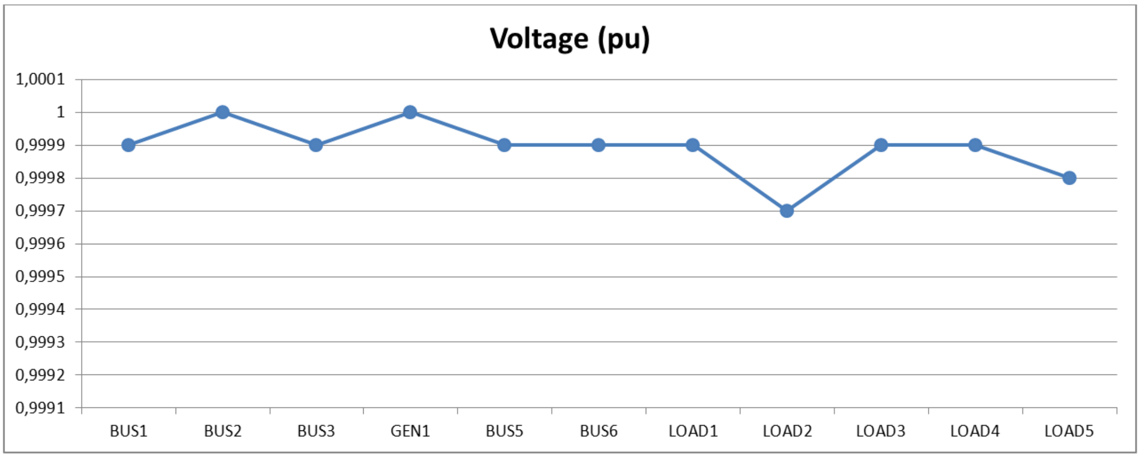

Figure 33 – Bus voltage profile in scenario 4 with centralized generation

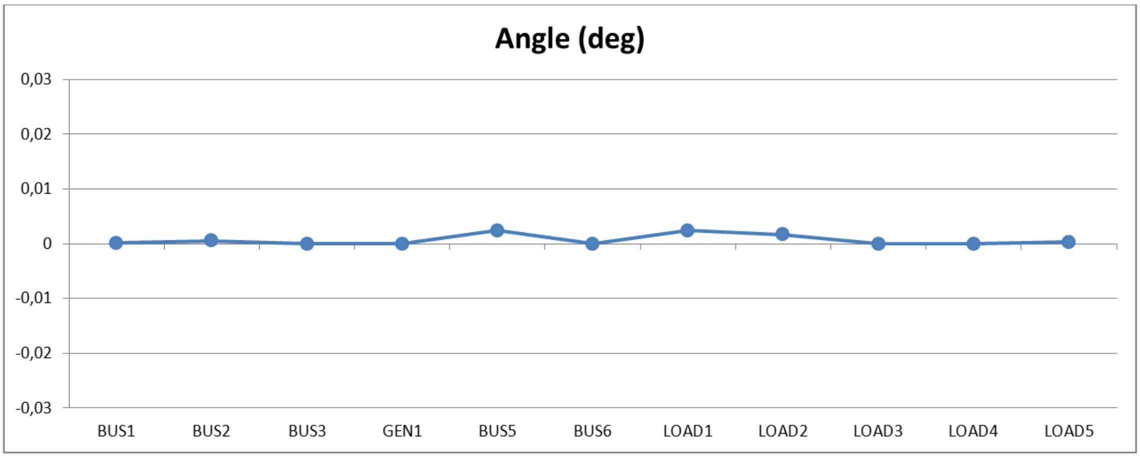

Figure 34 – Bus voltage angle in scenario 4 with centralized generation

As observed in figure 33 and table XXXII, this scenario obtained a slightly better bus voltage profile, because the MG is operating in islanded mode and only the high and medium priority loads are in operation. The lowest bus voltage value is 0.9997 pu in bus 8 (LOAD2). As listed in table XXXI, the generation group (GEN1) is at peak power delivering 300.1 kW of active power and 505.2 kVAr of reactive power. Bus GEN1 supplies the operating loads and acts as slack bus (swing bus), compensating losses and regulating the active and reactive power in the MG.

8.1.5. Case 5C

In this scenario, the MG is operating in islanded mode and only the high priority loads are connected to the grid. The five induction motors with a power demand of 250 kW are now supplied by the generation group (GEN1) at 70% of the peak power generation capacity (252 kW). This is the less favourable case and proper factory operation is only assured through a load-shedding technique. All the office equipment must be disconnected from the grid in order to prevent an interruption of supplied power to the crucial loads. Tables XXXIII and XXXIV show the results obtained from the power flow study for this scenario, and the bus voltage and angle profiles are shown in figures 35 and 36.

Table XXXIII – Network generator data

Generator	Bus	PGen (MW)	QGen (MVAr)
GEN1	4	0.2500	0.3336

Table XXXIV – Network bus data

Bus	Bus name	Base voltage (kV)	Voltage (pu)	Angle (deg)
1	BUS1	13.8	1.0000	0.00001
2	BUS2	0.480	1.0000	0.00008
3	BUS3	0.480	0.9999	-0.00009
4	GEN1*	0.480	1.0000	0
5	BUS5	0.480	1.0000	0.00008
6	BUS6	0.480	0.9999	-0.0001
7	LOAD1	0.480	1.0000	0.00008
8	LOAD2	0.208	1.0000	0.00008
9	LOAD3	0.208	0.9999	-0.0001
10	LOAD4	0.480	0.9999	-0.0001
11	LOAD5	0.480	0.9998	0.0002

* Bus GEN1 is defined as slack bus (swing bus)

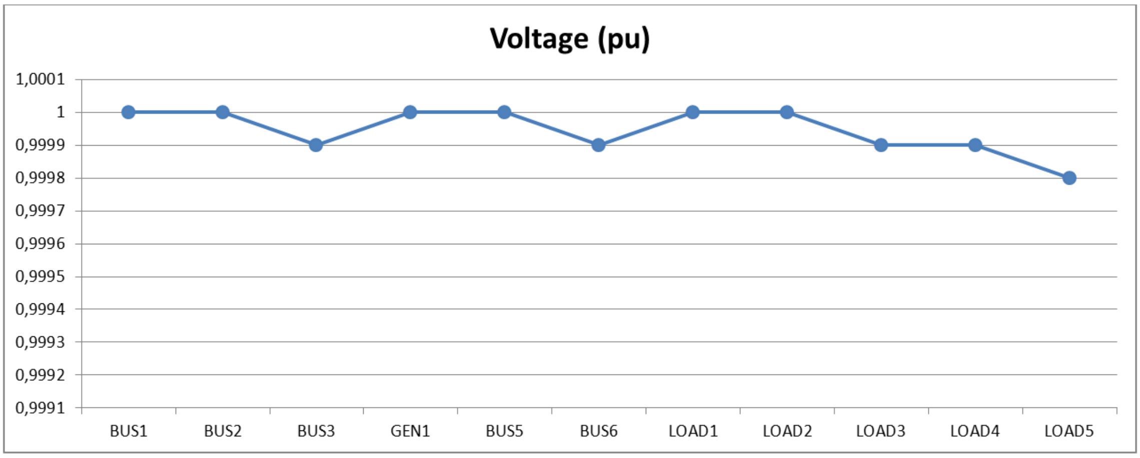

Figure 35 – Bus voltage profile in scenario 5 with centralized generation

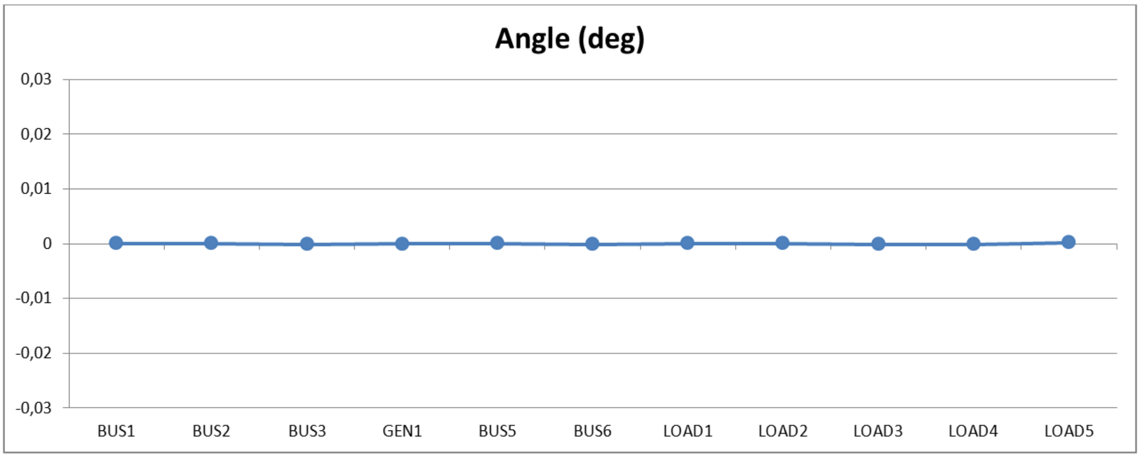

Figure 36 – Bus voltage angle in scenario 5 with centralized generation

As observed in figure 35 and table XXXIV, there is a slight improvement in the bus voltage profile obtained for this scenario when compared to the previous scenario 4C, since the high priority loads are the only loads that remain in operation. The lowest bus voltage value is now 0.9998 pu in bus 11 (LOAD5). As listed in table XXXIII, the generation group (GEN1) is at 70% of the peak power generation capacity delivering 250 kW of active power and 333.6 kVAr of reactive power. Bus GEN1 also needs to be defined as slack bus (swing bus) and supplies the high priority loads.

8.2. Decentralized MG

A decentralized MG architecture for this industrial site is represented in figure 37 and includes four generation groups located at the generation buses, GEN1, GEN2, GEN3 and GEN4. The generation groups act as uninterruptible power generators equipped with a bank of batteries dispersed along the grid and close to the higher priority loads. The branch and generator group data for this configuration are listed in tables XXXV and XXXVI.

Table XXXV – Cable data

Branch	Voltage (kV)	Load (kW)	Distance (m)	R (Ω)	X (Ω)
4 ↔ 2	0.480	10	30	0.0052	0.0026
5 ↔ 3	0.480	50	30	0.002	0.0027
2 ↔ 6	0.480	80	30	0.0052	0.0026
6 ↔ 8	0.480	15	10	0.024	0.0015
3 ↔ 7	0.480	320	30	0.002	0.0027
7 ↔ 11	0.480	60	40	0.0392	0.0064
7 ↔ 12	0.480	250	30	0.0023	0.0025
13 ↔ 12	0.480	250	10	0.0023	0.0025
14 ↔ 9	0.208	50	10	0.024	0.0015

Table XXXVI – Generator group data

Bus	Bus name	Bus voltage (kV)	Peak power (kW)
4	GEN1	0.480	10
5	GEN2	0.480	50
13	GEN3	0.480	250
14	GEN4	0.208	50

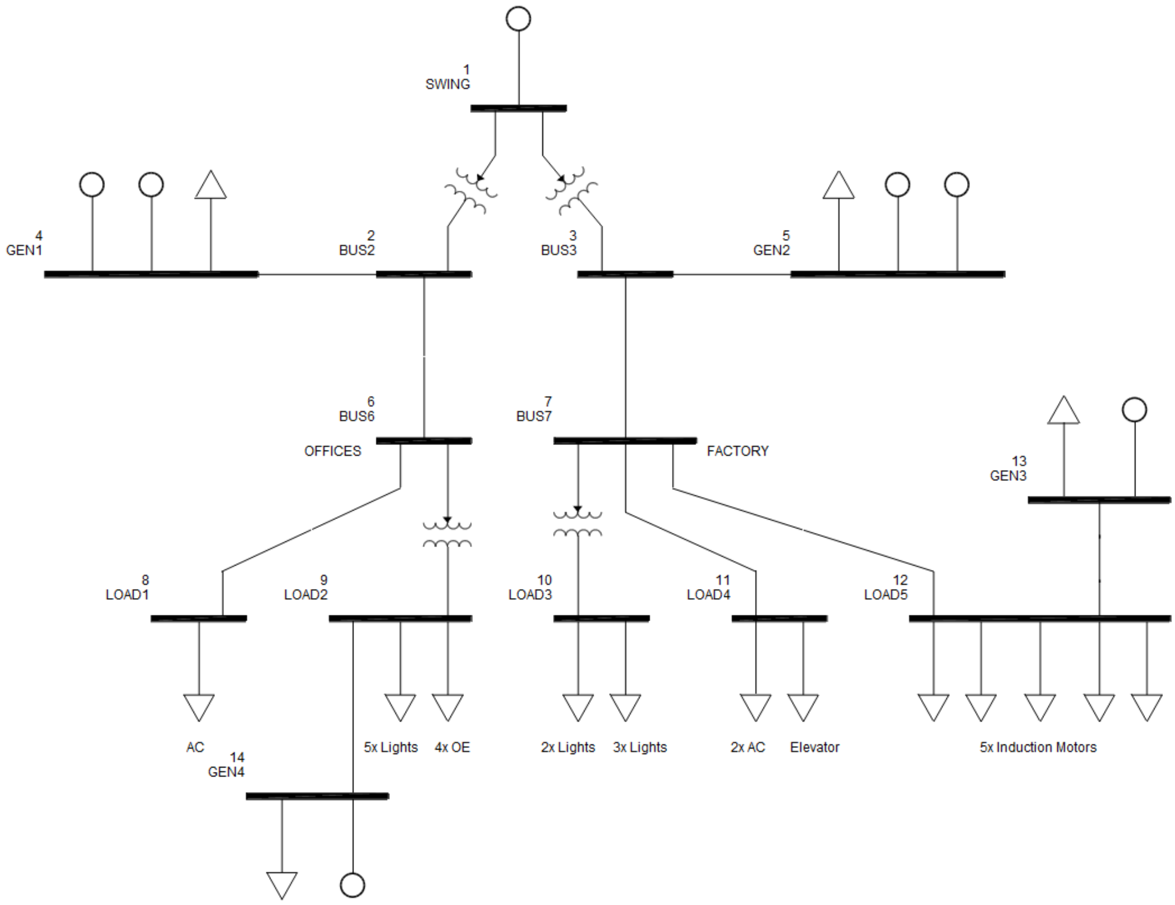

Figure 37 – Schematic of the MG with decentralized generation

8.2.1. Case 1D

In this scenario, the MG is connected to the public grid and both factory and offices are operating at full load (400 kW). The loads are supplied by the generation groups (GEN1, GEN2, GEN3 and GEN4) at peak power generation capacity (360 kW) and the public grid delivers the power needed to supply the remaining loads (40 kW). This represents the most satisfactory scenario during grid-connected operation mode, since all the generation groups are at their peak power and minimum power is imported from the public grid. Tables XXXVII and XXXVIII show the results obtained from the power flow study for this scenario, and the bus voltage and angle profiles are shown in figures 38 and 39.

Table XXXVII – Network generator data

Generator	Bus	PGen (MW)	QGen (MVAr)
Public grid	1	0.0402	0.0655
GEN1	4	0.0100	0.0675
GEN2	5	0.0500	0.1769
GEN3	13	0.2500	0.3529
GEN4	14	0.0500	0.2221

Table XXXVIII – Network bus data

Bus	Bus name	Base voltage (kV)	Voltage (pu)	Angle (deg)
1	SWING	13.8	1.0000	0
2	BUS2	0.480	1.0000	-0.0017
3	BUS3	0.480	1.0000	-0.0003
4	GEN1	0.480	1.0000	-0.0026
5	GEN2	0.480	1.0000	-0.0023
6	BUS6	0.480	1.0000	-0.0010
7	BUS7	0.480	0.9999	0.0004
8	LOAD1	0.480	1.0000	0.0016
9	LOAD2	0.208	0.9999	-0.0019
10	LOAD3	0.208	0.9996	0.0015
11	LOAD4	0.480	0.9998	0.0200
12	LOAD5	0.480	0.9999	0.0003
13	GEN3	0.480	1.0000	-0.0002
14	GEN4	0.208	1.0000	-0.0150

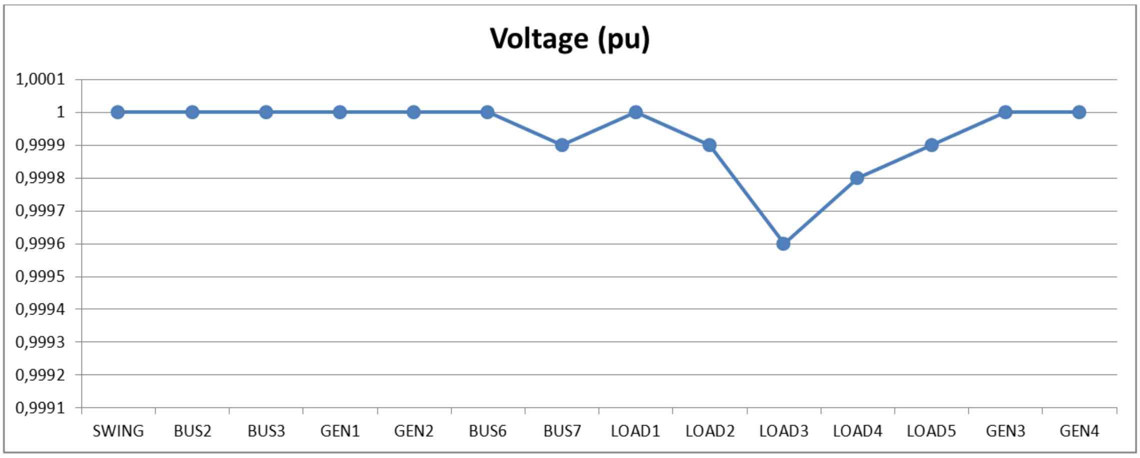

Figure 38 – Bus voltage profile in scenario 1 with decentralized generation

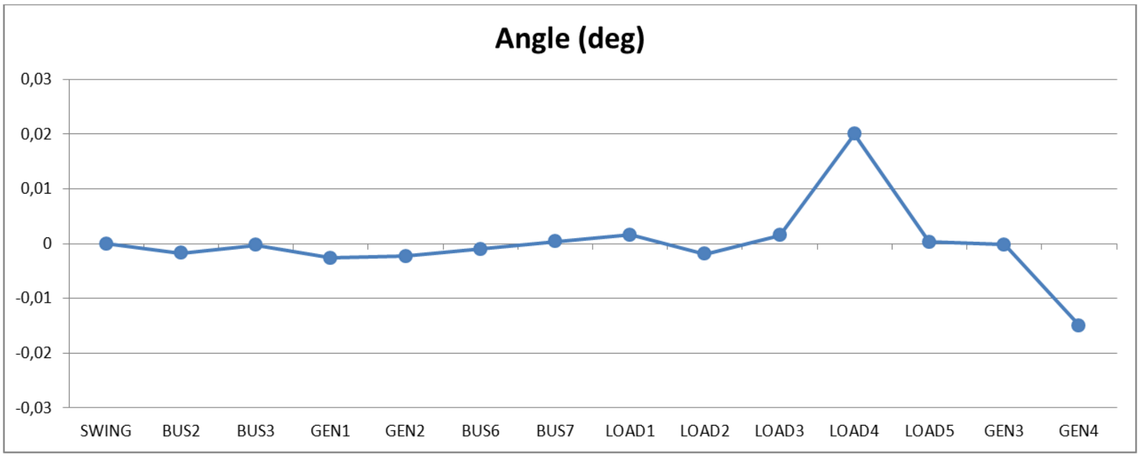

Figure 39 – Bus voltage angle in scenario 1 with decentralized generation

The bus voltage profile in figure 38 and values listed in table XXXVIII show improvements over the initial scenario. As observed, this scenario with decentralized generation obtained a relatively better bus voltage profile than scenario 1C with centralized generation. This is expected, since there are four generation groups dispersed along the grid to supply the loads. The lowest bus voltage value is now 0.9996 pu in bus 10 (LOAD3). As listed in table XXXVII, the generation groups (GEN1, GEN2, GEN3 and GEN4) are at their peak power delivering 360 kW of active power and 819.4 kVAr of reactive power, while the public grid delivers 40.2 kW and 65.5 kVAr needed to supply the loads and compensate losses.

8.2.2. Case 2D

In this scenario, the MG is connected to the public grid and both factory and offices are operating at full load (400 kW). However, the loads are now supplied by the generation groups (GEN1, GEN2, GEN3 and GEN4) at 50% of the peak power generation capacity (180 kW). In this less favourable case, the MG needs to import more power from the public grid to supply the loads (220 kW). Tables XXXIX and XL show the results obtained from the power flow study for this scenario, and the bus voltage and angle profiles are shown in figures 40 and 41.

Table XXXIX – Network generator data

Generator	Bus	PGen (MW)	QGen (MVAr)
Public grid	1	0.2202	0.0163
GEN1	4	0.0050	0.0543
GEN2	5	0.0250	0.1395
GEN3	13	0.1250	0.4305
GEN4	14	0.0250	0.2445

Table XL – Network bus data

Bus	Bus name	Base voltage (kV)	Voltage (pu)	Angle (deg)
1	SWING	13.8	1.0000	0
2	BUS2	0.480	1.0000	-0.0046
3	BUS3	0.480	1.0000	-0.0045
4	GEN1	0.480	1.0000	-0.0053
5	GEN2	0.480	1.0000	-0.0061
6	BUS6	0.480	1.0000	-0.0044
7	BUS7	0.480	0.9999	-0.0050
8	LOAD1	0.480	1.0000	-0.0017

9	LOAD2	0.208	1.0000	-0.0079
10	LOAD3	0.208	0.9996	-0.0039
11	LOAD4	0.480	0.9998	0.0146
12	LOAD5	0.480	0.9999	-0.0063
13	GEN3	0.480	1.0000	-0.0080
14	GEN4	0.208	1.0000	-0.0224

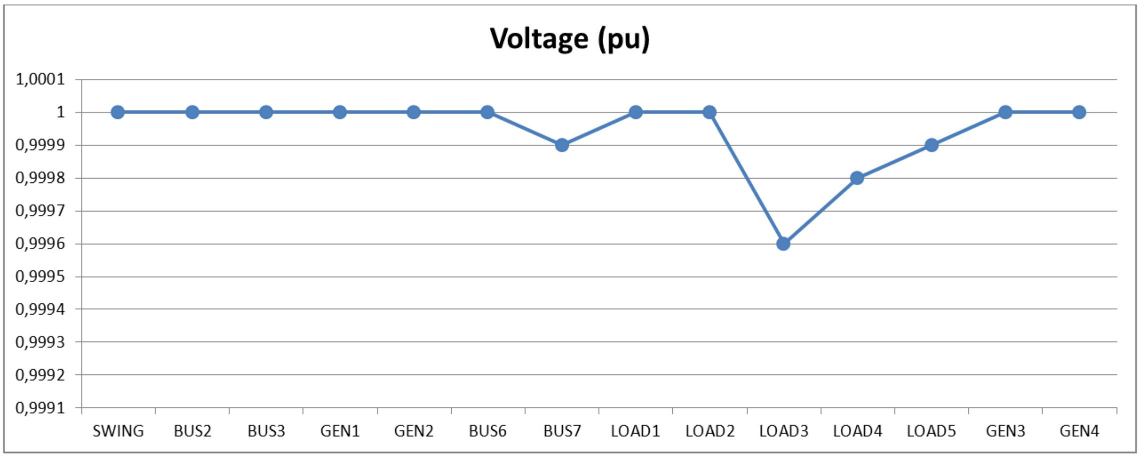

Figure 40 – Bus voltage profile in scenario 2 with decentralized generation

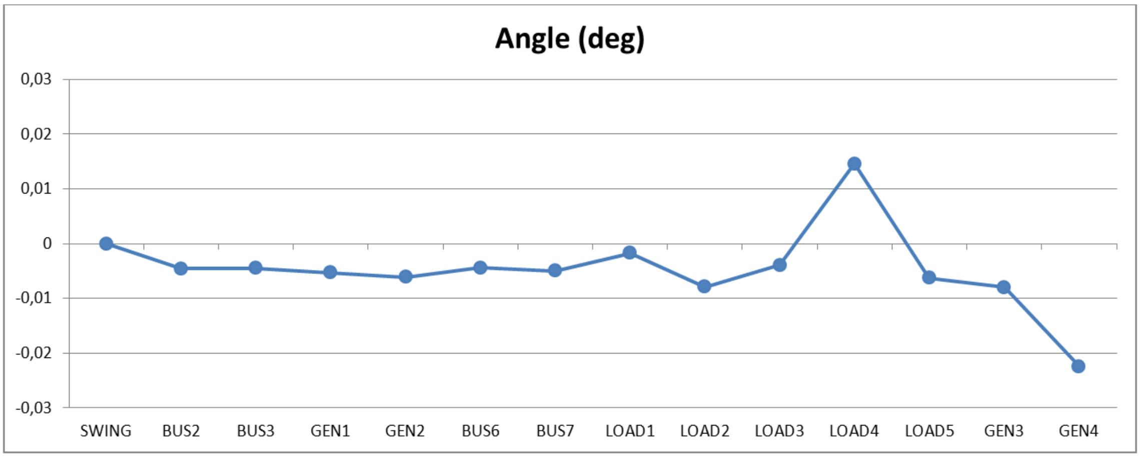

Figure 41 – Bus voltage angle in scenario 2 with decentralized generation

As expected, the bus voltage profile in figure 40 and bus voltage values listed in table XL show a noticeable improvement over the scenario 1C with centralized generation. The lowest bus voltage value is also 0.9996 pu in bus 10 (LOAD3). As listed in table XXXIX, the generation groups (GEN1, GEN2, GEN3 and GEN4) are at 50% of their peak power generation capacity delivering 180 kW of active power and 868.8 kVAr of reactive power, while the public grid delivers 220.2 kW and 16.3 kVAr needed to supply the loads and compensate losses.

8.2.3. Case 3D

In this scenario, the MG is also connected to the public grid. But the main factory and offices are now operating at 75% (240 kW) and 25% (20 kW), respectively. In the main factory, both air conditioning units and an induction motor are out of service. In the office, most of the lights and office equipment are not in use and the air conditioning unit is also out of service. The loads are supplied by the generation groups (GEN1, GEN2, GEN3 and GEN4) at 75% of the peak power generation capacity (270 kW). Tables XLI and XLII show the results obtained from the power flow study for this scenario, and the bus voltage and angle profiles are shown in figures 42 and 43.

Table XLI – Network generator data

Generator	Bus	PGen (MW)	QGen (MVAr)
Public grid	1	-0.0099	0.0544
GEN1	4	0.0075	0.0205
GEN2	5	0.0375	0.1230
GEN3	13	0.1875	0.2672
GEN4	14	0.0375	0.0439

Table XLII – Network bus data

Bus	Bus name	Base voltage (kV)	Voltage (pu)	Angle (deg)
1	SWING	13.8	1.0000	0
2	BUS2	0.480	1.0000	0.0024
3	BUS3	0.480	1.0000	-0.0002
4	GEN1	0.480	1.0000	0.0022
5	GEN2	0.480	1.0000	-0.0016
6	BUS6	0.480	1.0000	0.0029
7	BUS7	0.480	1.0000	0.0002
8	LOAD1	0.480	1.0000	0.0029
9	LOAD2	0.208	1.0000	0.0051
10	LOAD3	0.208	0.9996	0.0013
11	LOAD4	0.480	0.9999	0.0114
12	LOAD5	0.480	1.0000	0.0002
13	GEN3	0.480	1.0000	-0.0002
14	GEN4	0.208	1.0000	0.0026

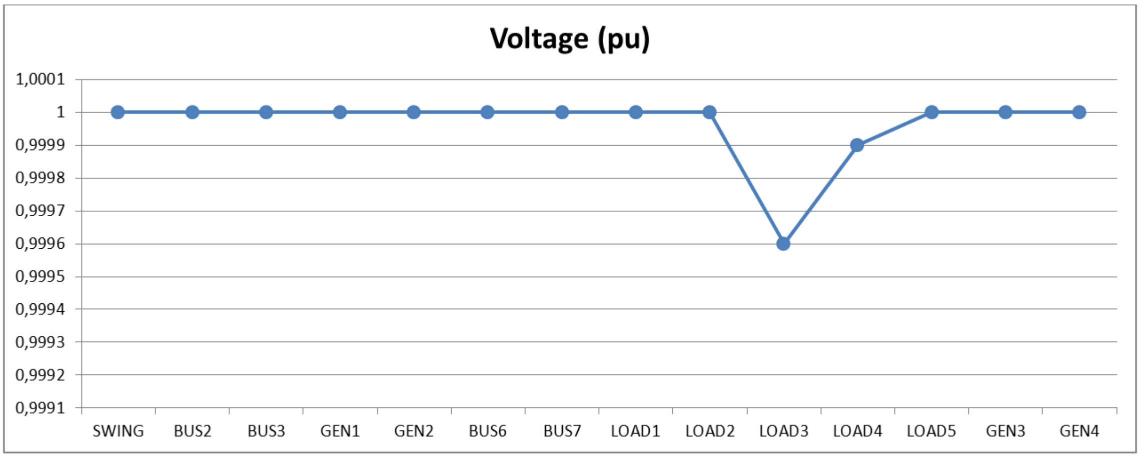

Figure 42 – Bus voltage profile in scenario 3 with decentralized generation

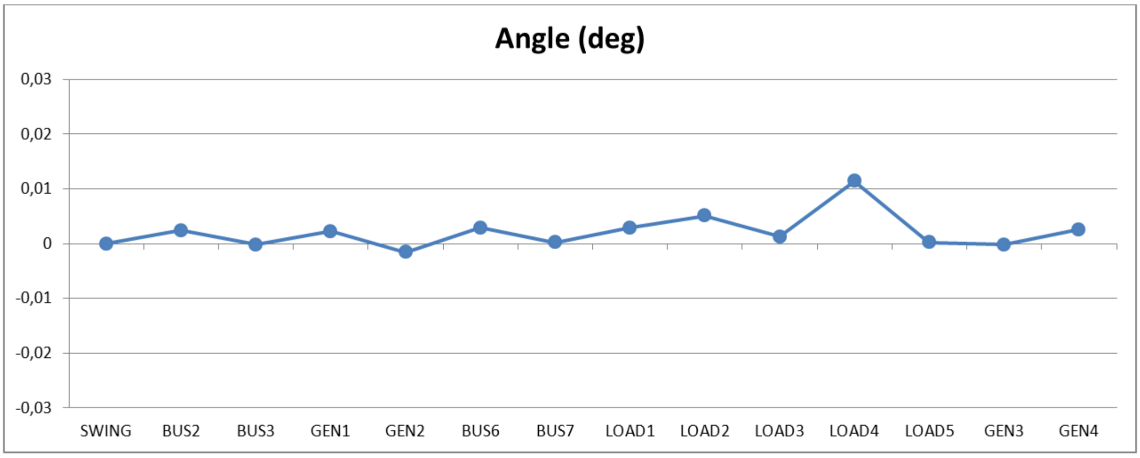

Figure 43 – Bus voltage angle in scenario 3 with decentralized generation

As expected, the bus voltage profile in figure 42 and bus voltage values listed in table XLII show a better bus voltage profile than scenario 3C with centralized generation. It can be also observed a slight improvement over the previous scenarios 1D and 2D due to a decrease in power demand. The lowest bus voltage value is 0.9996 pu in bus 10 (LOAD3). As listed in table XLI, the generation groups (GEN1, GEN2, GEN3 and GEN4) are at 75% of their peak power generation capacity delivering 270 kW of active power and 454.6 kVAr of reactive power. In this scenario, 9.9 kW of active power is also exported to the public grid.

8.2.4. Case 4D

In this scenario, there is no connection to the public grid. MG is operating in islanded mode and all the high and medium priority loads are connected to the grid. The five induction motors with a power demand of 250 kW and the office equipment with a power demand of 50 kW are supplied by the generation groups (GEN1, GEN2, GEN3 and GEN4) at peak power generation capacity (360 kW). This is the most satisfactory scenario during islanded operation mode, since all the generation groups are operating at their power peak and the higher priority loads can remain in operation. Tables XLIII and XLIV show the results obtained from the power flow study for this scenario, and the bus voltage and angle profiles are shown in figures 44 and 45.

Table XLIII – Network generator data

Generator	Bus	PGen (MW)	QGen (MVAr)
GEN1	4	0.0100	0.0370
GEN2	5	0.0500	0.0702
GEN3	13	0.1900	0.2592
GEN4	14	0.0500	0.1387

Table XLIV – Network bus data

Bus	Bus name	Base voltage (kV)	Voltage (pu)	Angle (deg)
1	BUS1	13.8	1.0000	0.0005
2	BUS2	0.480	1.0000	0.0013
3	BUS3	0.480	1.0000	0.0003
4	GEN1	0.480	1.0000	0.0009
5	GEN2	0.480	1.0000	-0.0003
6	BUS6	0.480	1.0000	0.0018
7	BUS7	0.480	1.0000	0.0002
8	LOAD1	0.480	1.0000	0.0018
9	LOAD2	0.208	0.9999	0.0025
10	LOAD3	0.208	1.0000	0.0025
11	LOAD4	0.480	1.0000	0.0025
12	LOAD5	0.480	1.0000	0.0003
13	GEN3*	0.480	1.0000	0
14	GEN4	0.208	1.0000	-0.0056

* Bus GEN3 is defined as slack bus (swing bus)

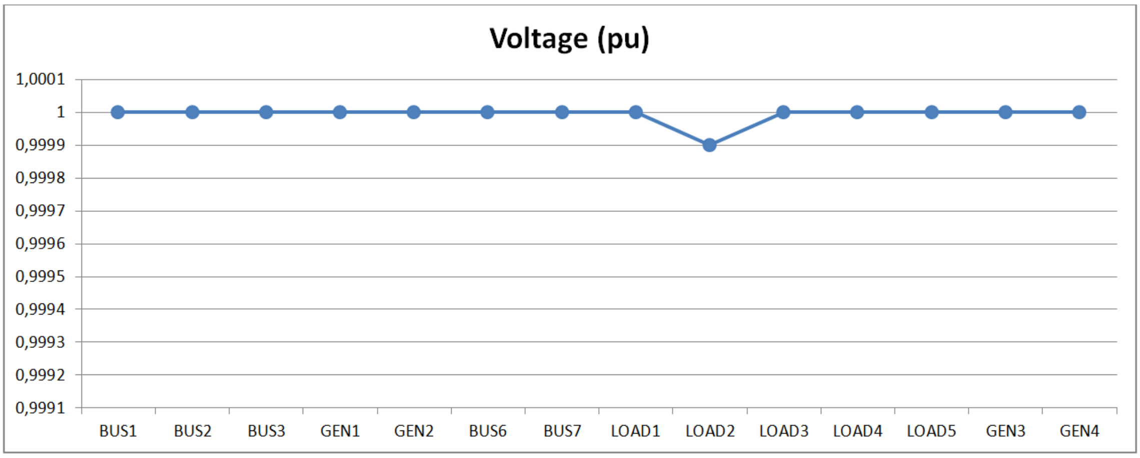

Figure 44 – Bus voltage profile in scenario 4 with decentralized generation

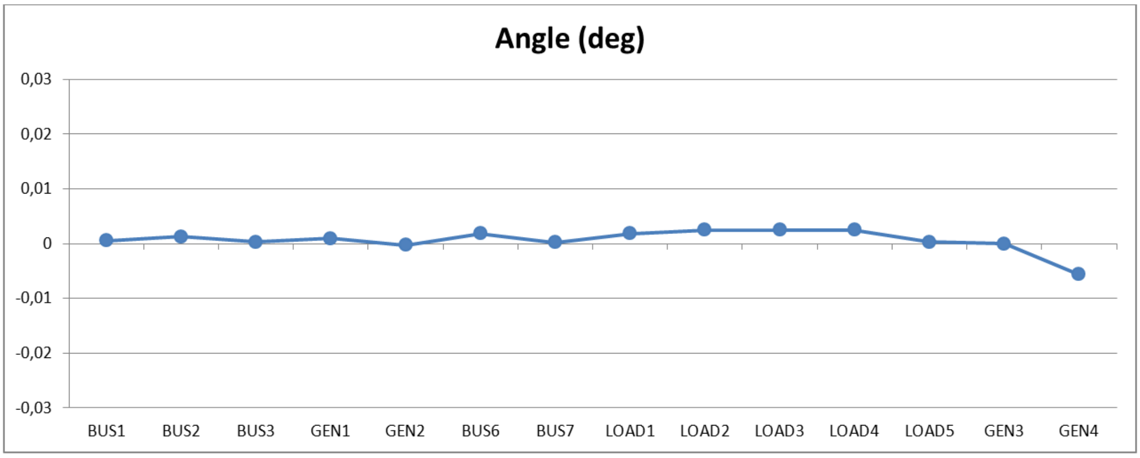

Figure 45 – Bus voltage angle in scenario 4 with decentralized generation

This scenario obtained bus voltages of exactly 1 pu for all buses with the exception of 0.9999 pu in bus 9 (LOAD2), as observed in figure 44 and table XLIV. This shows an improvement over the scenario 4C, because there are several generation groups supplying the high and medium priority loads. As listed in table XLIII, the dispersed generation groups (GEN1, GEN2, GEN3 and GEN4) are at their peak power delivering 300 kW of active power and 505.1 kVAr of reactive power. The bus GEN3 is defined as slack bus (swing bus) and regulates the active and reactive power in the MG.

8.2.5. Case 5D

In this scenario, the MG is operating in islanded mode and only the high priority loads are connected to the grid. The five induction motors with a power demand of 250 kW are now supplied by the generation groups (GEN1, GEN2, GEN3 and GEN4) at 70% of the peak power generation capacity (252 kW). This is the less favourable case and proper factory operation is only assured through a load-shedding technique. All the office equipment must be disconnected from the grid in order to prevent an interruption of supplied power to the crucial loads. Tables XLV and XLVI show the results obtained from the power flow study for this scenario, and the bus voltage and angle profiles are shown in figures 46 and 47.

Table XLV – Network generator data

Generator	Bus	PGen (MW)	QGen (MVAr)
GEN1	4	0.0070	0.0272
GEN2	5	0.0350	0.0725
GEN3	13	0.1730	0.2644
GEN4	14	0.0350	-0.0307

Table XLVI – Network bus data

Bus	Bus name	Base voltage (kV)	Voltage (pu)	Angle (deg)
1	BUS1	13.8	1.0000	0.0018
2	BUS2	0.480	1.0000	0.0056
3	BUS3	0.480	1.0000	0.0007
4	GEN1	0.480	1.0000	0.0053
5	GEN2	0.480	1.0000	-0.00002
6	BUS6	0.480	1.0000	0.0063
7	BUS7	0.480	1.0000	0.0005
8	LOAD1	0.480	1.0000	0.0063
9	LOAD2	0.208	1.0000	0.0100

10	LOAD3	0.208	1.0000	0.0005
11	LOAD4	0.480	1.0000	0.0005
12	LOAD5	0.480	1.0000	0.0004
13	GEN3*	0.480	1.0000	0
14	GEN4	0.208	1.0000	0.0120

* Bus GEN3 is defined as slack bus (swing bus)

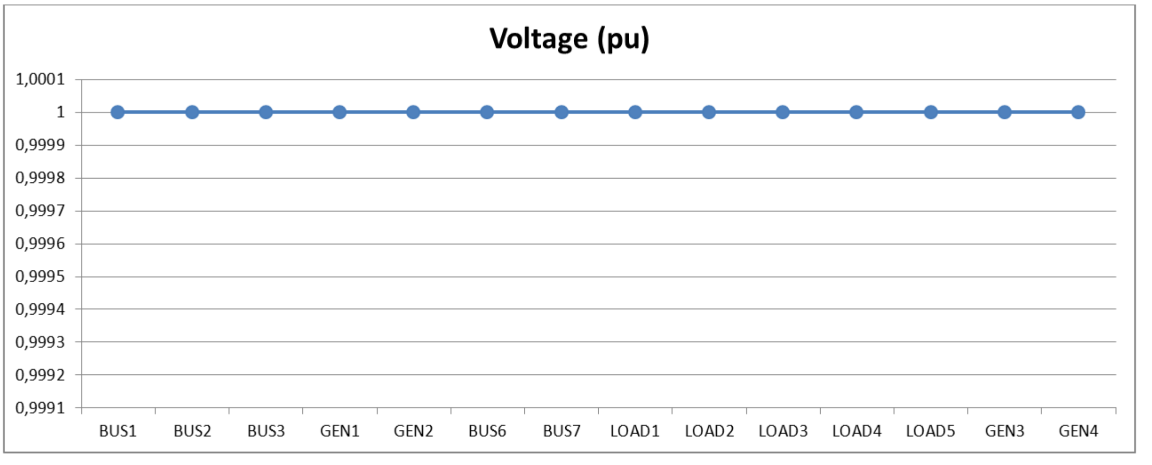

Figure 46 – Bus voltage profile in scenario 5 with decentralized generation

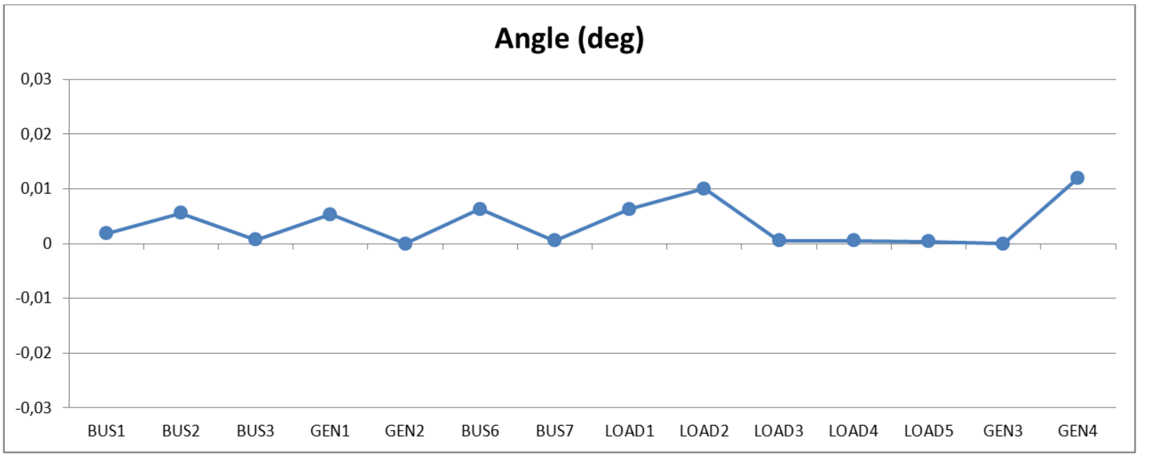

Figure 47 – Bus voltage angle in scenario 5 with decentralized generation

This scenario obtained bus voltages of exactly 1 pu for all grid buses, as observed in figure 46 and table XLVI. This is expected, since the dispersed generation groups only supply the high priority loads. As listed in table XLV, the dispersed generation groups (GEN1, GEN2, GEN3 and GEN4) are at 70% of their peak power generation capacity delivering 250 kW of active power and 333.4 kVAr of reactive power. The bus GEN3 is also defined as slack bus (swing bus).

8.3. Fault analysis

In the event of an external fault such as a fault in the MV feeder or distribution transformer of the public grid, the fault is dealt with by the public grid protection system. The MG isolation is made by a switch or circuit breaker located at the PCC in case of no public grid protection tripping. Both centralized and decentralized MG configurations can effectively respond to external fault events. However, in the event of an internal fault located in one of the LV feeders, centralized and decentralized configurations will perform differently. Figures 48 and 49 show the centralized and decentralized MG with two internal faults (F1 and F2).

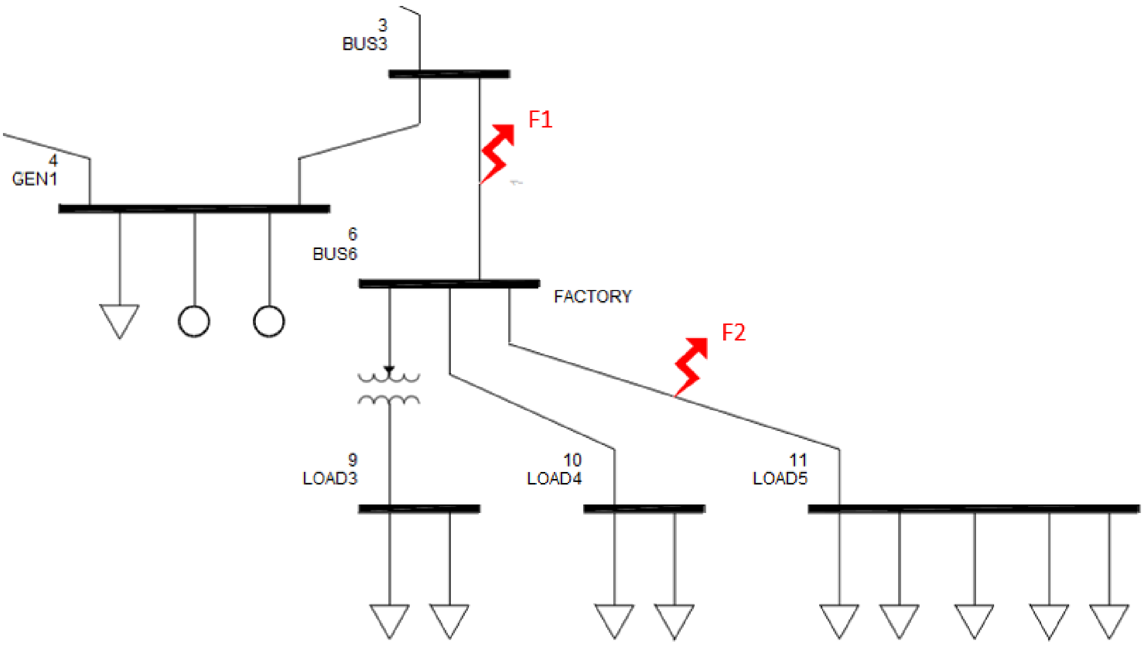

Figure 48 – Centralized MG with internal faults F1 and F2

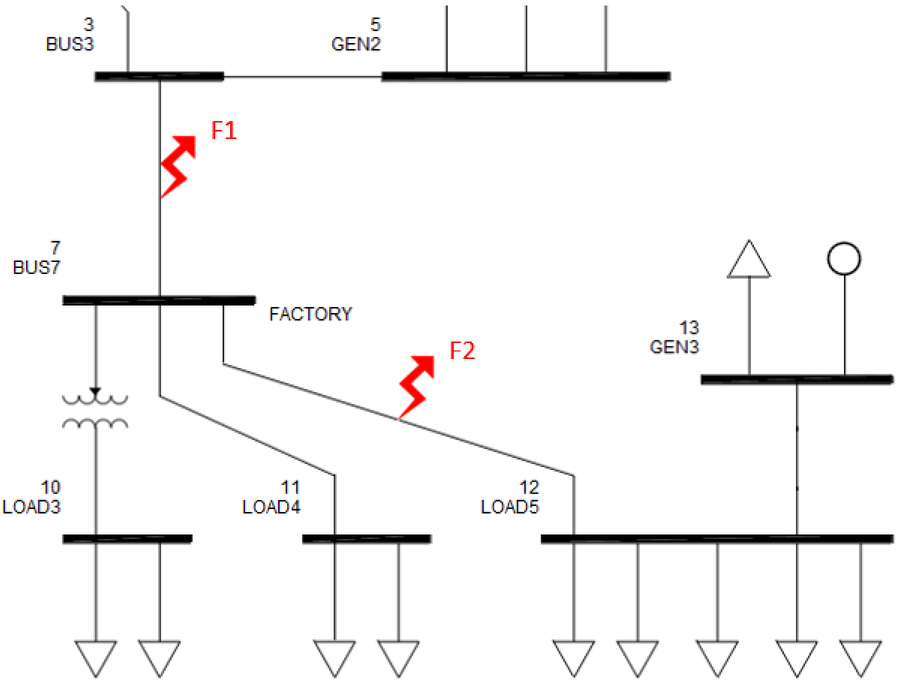

Figure 49 – Decentralized MG with internal faults F1 and F2

The internal faults F1 and F2 are located in branches that supply a bus with crucial loads (LOAD5). In the configuration with centralized generation shown in figure 48, a fault F1 in the branch from bus number 3 (BUS3) to bus number 6 (BUS6) and a fault F2 in the branch from bus number 6 (BUS6) to bus number 11 (LOAD5) cause a power interruption to the crucial loads. The centralized MG has a single generation group that supplies the factory and office loads, making this architecture unable to deal with internal faults in feeders that supply crucial loads. Moreover, a critical fault in the generation group bus (GEN1) may lead to the total MG outage during islanded operation mode. In the configuration with decentralized generation shown in figure 49, a fault F1 in the branch from bus number 3 (BUS3) to bus number 7 (BUS7) and a fault F2 in the branch from bus number 7 (BUS7) to bus number 12 (LOAD5) may not cause a total power interruption in the crucial loads. This architecture offers more flexibility to isolate internal faults due to the dispersed generation units connected to the MG in different strategic locations. The generation group (GEN3) is located near the crucial loads, providing a backup power supply during island operation mode and enabling the crucial loads to remain in operation when a fault F1 or F2 occurs. Also, in the event of a faulty generation group, the crucial loads can be continuously supplied by the remaining generation groups.

8.3.1. Short-circuit analysis

The short-circuit analysis presented in this section is based on the symmetrical (three-phase) and asymmetric faults (phase-earth PE) at F1 and F2, as represented in figures 48 and 49. The faults F1 and F2 are both assumed to happen at half the impedance point of the respective network component, at the low voltage level of 480 V. This analysis adopts the approximate method based on the calculation of the equivalent impedance seen from the fault point. The impedance is obtained from the single-phase wiring diagram of the study presented in [84, 85]. The network parameters were considered as constant and the contribution of the induction motors on feeding faults in the transient period is neglected. The short-circuit apparent power, Scc, of the public grid at BUS1 is 250 MVA and the ratio of the reactance and resistance is Xcc/Rcc=6.

Table XLVII presents the values of the expected short-circuit currents for the two types of defect considered. The maximum short-circuit power to be supplied by the set of inverters of each generator group corresponds to 150% of its peak power [86]. In the calculation of phase to line-to-earth fault currents (1Ph), it was considered that:

- The zero-impedance of the transformers assumes the same value of its direct impedance;
- The zero-sequence impedance of the inverters was neglected (inverters that emulate zero-sequence parameters).

Table XLVII – Fault current results (Amp): Symmetric (3Ph) and Asymmetric (1Ph)

Fault type	**Fault location**	**Public Grid**	**Centralized MG**		**Decentralized MG**	
			On-Grid	**Off-Grid**	**On-Grid**	**Off-Grid**
3Ph	**F1**	19779	19919	648	20057	1116
	F2	16167	16204	645	16387	1119
1Ph	**F1**	7346	9017	324	7537	581
	F2	6294	7467	322	6477	594

The analysis of this table shows that:

- Symmetric and asymmetric faults generate significant currents whenever the installation is connected to the public grid (On-Grid mode). The fault currents increase slightly with the integration of the generator groups (Centralized MG / Decentralized MG);
- Symmetrical short-circuit currents for MGs in island mode are substantially low. In Centralized MG, these fault currents are around 1.4 times the normal current at rated load (Is). In Decentralized MG, these fault currents are around 2.4×Is;
- Asymmetric faults, Ph-PE, in MGs in island mode generate very low currents. For example, in the case of Centralized MG these currents correspond to about 0.85 of Is (at fault F2) and in Decentralized MG are around 1.3×Is (at fault F1).

Thus it is possible to say that the regulation of short-circuit protections in MGs operating in grid-connected mode is relatively straight-forward. On another hand, the regulation of short-circuit protections in islanded MGs is quite more difficult.

8.4. Comments

In scenarios where the MG is in grid-connected operation mode, the public grid acts as a generator connected to the slack or swing bus (SWING/BUS1) and it balances the active and reactive power by setting the voltage angle reference for all MG buses. When the MG is disconnected from the public grid (case 4C/4D and 5C/5D) and there is no slack or swing bus available, the MG bus connected to the generator with the largest capacity becomes the new swing bus and it is now responsible for regulating the active and reactive power. Given the small proportions of the industrial grid studied, the voltage and angle values obtained for each bus do not vary much between the different scenarios and it is merely a result of a decrease in load demand. This can be easily observed in the islanded operation scenarios (case 4C/4D and 5C/5D), there is an improvement in the bus voltage profiles for both MG configurations because only the crucial loads are being supplied.

Besides, it is noticeable few variations between the results obtained from the centralized MG and decentralized MG configurations. When comparing the bus voltage profiles in every scenario, the MG with dispersed generation groups obtained slightly better results than the MG with a single generation group. As expected, the decentralized MG provides better quality of supplied power to the loads with slightly better bus voltage profiles, since there are generation groups dispersed along the grid and located near the crucial and most demanding loads. Moreover, the decentralized MG configuration also provides flexibility to isolate faults in branches that supply crucial loads and ensures the continuous power supply in the event of a faulty generation group. On the other hand, there is bi-directional power flow in the decentralized MG configuration, which increases the protection system requirements. The centralized MG configuration is slightly simpler to implement and requires less protection devices, but it does not provide the flexibility required to ensure the continuous operation of crucial loads during islanded mode. Figure 50 represents the schematics of the industrial MG with centralized and decentralized generation.

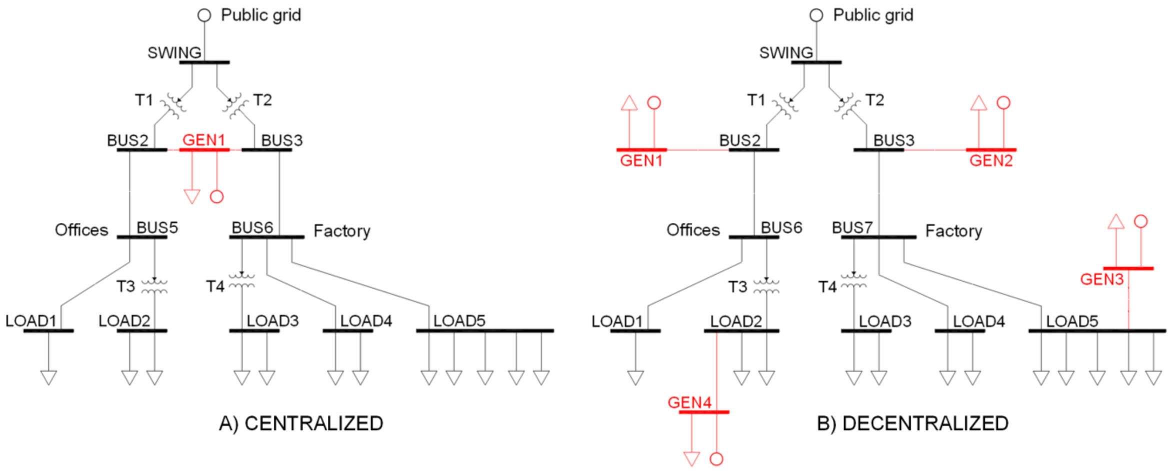

Figure 50 – Schematic of the industrial MG: A) centralized and B) decentralized

Table XLVIII shows a brief comparison between the two architecture configurations based on the aspects previously mentioned in this section.

Table XLVIII – Comparison between centralized and decentralized generation

	Advantages	Disadvantages
Centralized	• Simple and less expensive implementation • Less protection devices and power converter interfaces	• Difficulty in isolating internal faults
Decentralized	• Increased power quality and less transmission losses • Flexibility to isolate internal faults	• High protection requirement due to bi-directional power flow

9. CONCLUSIONS

This work addressed some of the most important aspects to assist in the study of industrial MG architectures. These aspects included a brief overview of the industrial sector and definition of the MG concept, as well as a characterization of control and communication architectures, energy resources, control strategies for power converters and protection systems in MGs. The overview of the industrial sector focused on the challenge of implementing energy efficiency measures in SMEs due to their limited financial resources and lack of knowledge regarding cost-efficient applications of RES. Taking this into account, implementing MGs in small scale enterprises might not be an easy and simple task to accomplish, given the innumerable barriers these enterprises come across. Both the control and communication architectures can follow a centralized or decentralized configuration. There are economic concerns associated with the architecture configuration, because a centralized approach proposes simpler and thus cheaper local control devices, and also a central controller in charge of processing data and making decisions. A decentralized approach requires more advanced and complex local control devices, increasing the system cost. Moreover, the communication architecture may follow a wired or wireless infrastructure based on a wide range of wired or wireless technologies with different characteristics. The choice of an appropriate communication technology for a MG must be according to the installation costs and system specifications. Environmental concerns led to the deployment of several types of clean energy sources in MGs. The overview of these energy sources mainly focused on solar and wind power generation systems. PV technologies have been through a decrease in module prices and offer a long service life with low operation costs, but the availability of PV and wind power systems is dependent on the location and weather conditions. It is suggested the integration of hybrid generation systems into the grid to ensure the continuous power supply and thus overcome the dependency problem of PV and wind power systems. Most of the energy sources require power converter interfaces to connect with the grid and these power converters may follow different control strategies. The master-slave approach might not be suited for systems with dispersed generation, since a higher communication requirement is needed. The multi-master approach provides an increase in reliability and allows simple system expansion. An effective protection system is important to ensure a safe MG operation, as well as the safety of crucial loads, generation sources, storage units and people. The overview of the protection systems for feeders, buses and generation units focused on the differential protection, mainly because this strategy overcomes the problem caused by the integration of intermittent generation units into the grid. The earthing protection systems commonly adopted in LV distribution systems is also addressed. The study concluded that among the available systems, TN-S is the preferred earthing system for MGs.

The case study of a small scale centralized and decentralized MG was made using the PSS/E Xplore software from Siemens. Both MG architectures showed almost ideal bus voltage results (approximately 1 pu) due to the small grid size. However, the bus voltage profiles obtained from the power flow study showed relatively better results with the decentralized MG. In addition, it concluded that a decentralized MG is more capable of isolating internal faults without compromising the operation of the crucial loads, due to a dispersed deployment of generation units along the grid and close to loads. However, because of bi-directional power flow, the decentralized approach has a higher protection requirement, increasing the system costs. Taking into account the financial limitations of smaller enterprises, every increase in system cost needs to be carefully considered. In contrast, a centralized approach is simpler and cheaper to implement, but it cannot isolate internal faults without compromising the continuous operation of crucial loads. A centralized deployment of the generation units might be the preferred solution for small grids. With a significant increase in grid size and number of loads, a decentralized deployment of several generation units along the grid may bring noticeable advantages in flexibility and quality of supplied energy. Furthermore, the operation of MGs in island mode can be problematic. It was shown that currents generated by symmetric and asymmetric faults in island operation mode are substantially lower than in grid-connected operation. Therefore, in situations of minimum short-circuit currents setting the right protections is neither simple nor economical.

Future work and additional notes:

This dissertation was based on the project report made for the first INDuGRID project task, entitled “*Evaluating Architectures of Industrial Microgrids*”. Additional aspects from two papers submitted to the ICEREGA’17 conference were also included in this work. Both conference papers are available in Appendix B. In addition, research work was developed regarding the second INDuGRID project task “*Protocols for guaranteeing zero net energy industries*”, but it was left for future work due to its incomplete state.

REFERENCES

[1] U. Salahuddin, A. Berthold, “Design and development of industrial microgrids”, White paper ABB, 2015.

[2] W. Muneer, K. Bhattacharya and C. A. Canizares, “Large-Scale Solar PV Investment Models, Tools and Analysis: The Ontario Case”, *IEEE Transactions on Power Systems*, vol. 26, n. 4, pp. 2547-2555, Nov. 2011.

[3] C. Genao, A. St. Leger, “Insight into Demand Response and Photovoltaic Source with Time of Day Pricing”, *Proceedings of the 2012 PES Transmission and Distribution Conference and Exposition*, pp. 1-8, May 2012.

[4] International Energy Outlook 2016, U.S. Energy Information Administration, May 2016. [Available online: https://www.eia.gov/outlooks/ieo/pdf/0484(2016).pdf (Accessed: 2017-02-24)]

[5] “Study on Energy Efficiency and Energy Saving Potential in Industry and on Possible Policy Mechanisms”, ICF International, Dec 2015. [Available online: https://ec.europa.eu/energy/sites/ener/files/documents/151201%20DG%20ENER%20Industrial%20EE%20study%20-%20final%20report_clean_stc.pdf (Accessed: 2017-09-14)]

[6] “Small and Medium-sized Enterprises: Local Strength, Global Reach”, Organisation for Economic Co-operation and Development (OECD), Jun. 2000. [Available online: http://www.oecd.org/cfe/leed/1918307.pdf (Accessed: 2017-02-01)]

[7] “Accelerating Energy Efficiency in Small and Medium-sized Enterprises”, International Energy Agency (IEA), 2015. [Available online: https://www.iea.org/publications/freepublications/publication/SME_2015.pdf (Accessed: 2017-02-01)]

[8] "Research to Access the Barriers and Drivers to Energy Efficiency in Small and Medium Sized Enterprises", UK Department of Energy & Climate Change, Nov. 2014. [Available online: https://www.gov.uk/government/uploads/system/uploads/attachment_data/file/392908/Barriers_to_Energy_Efficiency_FINAL_2014-12-10.pdf (Accessed: 2017-02-01)]

[9] M. Bröckl, J. Illman, L. Oja, I. Vehviläinen, "Energy Efficiency in Small and Medium Sized Enterprises", Nordic Council of Ministers, 2014.

[10] "World Energy Outlook Special Report: Energy and Climate Change", International Energy Agency (IEA), 2015. [Available online: https://www.iea.org/publications/freepublications/publication/WEO2015SpecialReportonEnergyandClimateChange.pdf (Accessed: 2017-03-08)]

[11] "Demand Response as a Power System Resource", Regulatory Assistance Project (RAP), May 2013. [Available online: http://www.raponline.org/wp-content/uploads/2016/05/synapse-hurley-demandresponseasapowersystemresource-2013-may-31.pdf (Accessed: 2017-09-25)]

[12] "Empowering Customer Choice in Electricity Markets", International Energy Agency (IEA), Oct. 2011. [Available online: https://www.iea.org/publications/freepublications/publication/Empower.pdf (Accessed: 2017-09-26)]

[13] "Benefits of Demand Response in Electricity Markets and Recommendations for Achieving Them", U.S. Department of Energy, Feb. 2006. [Available online: https://eetd.lbl.gov/sites/all/files/publications/report-lbnl-1252d.pdf (Accessed: 2017-09-26)]

[14] N. Hatziargyriou, "Microgrids: Architectures and Control", Wiley-IEEE press, 2014.

[15] J. C. Vasquez, J. M. Guerrero, E. Gregorio, P. Rodriguez, R. Teodorescu, and F. Blaabjerg, "Adaptive Droop Control Applied to Distributed Generation Inverters Connected to the Grid", *Proceedings of the 2008 IEEE International Symposium on Industrial Electronics*, pp. 2420-2425, 2008.

[16] J. C. Vasquez, J. M. Guerrero, A. Luna, P. Rodriguez, and R. Teodorescu, “Adaptive Droop Control Applied to Voltage-Source Inverters Operating in Grid-Connected and Islanded Modes”, *IEEE Transactions on Industrial Electronics*, vol. 56, no. 10, pp. 4088-4096, Oct. 2009.

[17] J. Kennedy, P. Ciufo, A. Agalgaonkar, “Intelligent Load Management in Microgrids”, *Proceedings of the 2012 IEEE Power and Energy Society General Meeting*, pp. 1-8, Jul. 2012.

[18] http://www.cleanspark.com/the-grid-perfection-a-new-microgrid-landscape-in-the-making/

[19] S. M. Nosratabadi, R. A. Hooshmand, E. Gholipour, “A comprehensive review on microgrid and virtual power plant concepts employed for distributed energy resources scheduling in power systems”, *Renewable and Sustainable Energy Reviews*, vol. 67, pp. 341-363, 2017.

[20] J. M. Guerrero, J. C. Vasquez, J. matas, L. G. de Vicuna and M. Castilha, “Hierarchical Control of Droop-Controlled AC and DC Microgrids—A General Approach Toward Standardization”, *IEEE Transactions on Industrial Electronics*, vol. 58, no. 1, pp. 158-172, Jan. 2011.

[21] K. D. Brabandere, B. Bolsens, J. V. D. Keybus, A. Woyte, J. Driesen, R. Belmans, “A Voltage and Frequency Droop Control Method for Parallel Inverters”, *IEEE Transactions on Power Electronics*, vol. 22, no. 4, pp. 1107-1115, Jul. 2007.

[22] A. M. Bollman, “An Experimental Study of Frequency Droop Control in a Low-Inertia Microgrid”, Master Thesis, University of Illinois, 2009.

[23] A. Bidram and A. Davoudi, “Hierarchical Structure of Microgrids Control System”, *IEEE Transactions on Smart Grid*, vol. 3, no. 4, pp. 1963-1976, Dec. 2012.

[24] O. Palizban, K. Kauhaniemi, “Hierarchical control structure in microgrids with distributed generation: Island and grid-connected mode”, *Renewable and Sustainable Energy Reviews*, vol. 44, pp. 797-813, 2015.

[25] L. K. Siow. P. L. So, H. B. Gooi, F. L. Luo, C. J. Gajanayake, Q. N. Vo, “Wi-Fi Based Server in Microgrid Energy Management System”, *Proceedings of the 2009 IEEE Region 10 Conference*, pp. 1-5, Jan. 2009.

[26] S. Shukla, Y. Deng, S. Shukla, L. Mili, "Construction of a Microgrid Communication Network", *IEEE Power Engineering Society Innovative Smart Grid Technology Conference*, pp. 1-5, Feb. 2014.

[27] A. Bani-Ahmed, L. Weber, A. Nasiri, H. Hosseini, "Microgrid Communications: State of the Art and Future Trends", *Proceedings of the 3rd International Conference on Renewable Energy Research and Applications*, pp. 780-785, Oct. 2014.

[28] P. P. Parikh, M. G. Kanabar, T. S. Sidhu, "Opportunities and Challenges of Wireless Communications Technologies for Smart Grid Applications", *Proceedings of the 2010 IEEE PES General Meeting*, pp. 1-7, Jul. 2010.

[29] E. Ancillotti, R. Bruno, M. Conti, "The role of communication systems in smart grids: Architectures, technical solutions and research challenges", *Computer Communications*, vol. 36, pp. 1665-1697, 2013.

[30] M. Kuzlu, M. Pipattanasomporn, S. Rahman, "Communication network requirements for major smart grid applications in HAN, NAN and WAN", *Computer Networks*, vol. 67, pp. 74-88, 2014.

[31] V. C. Gungor, D. Sahin, T. Kocak, S. Ergut, C. Buccella, C. Cecati, G. P. Hancke, "Smart Grid Technologies: Communication Technologies and Standards", *IEEE Transactions on Industrial Informatics*, vol. 7, no. 4, pp. 529-539, Nov. 2011.

[32] Z. Zhu, S. Lambothran, W. Chin, Z. Fan, "Overview of demand management in smart grid and enabling wireless communication technologies", *IEEE Wireless Communications*, vol. 19, no. 3, pp. 48-56, Jun. 2012.

[33] A. Usman, S. H. Shami, "Evolution of Communication Technologies for Smart Grids Applications", *Renewable and Sustainable Energy Reviews*, vol. 19, pp. 191-199, 2013.

[34] Z. Ding, W. J. Lee, "A Stochastic Microgrid Operation Scheme to Balance Between System Reliability and Greenhouse Gas Emissions", *IEEE Transactions on Industry Applications*, vol. 52, no. 2, pp. 1157-1166, Mar. 2016.

[35] L. Mariam, M. Basu, M. F. Conlon, "A Review of Existing Microgrid Architectures" *Journal of Engineering*, pp. 1-8, 2013.

[36] F. Katiraei, R. Iravani, N. Hatziargyriou, A. Dimeas, "Microgrids Management", *IEEE Power and Energy Magazine*, vol. 6, no. 3, pp. 66-77, 2008.

[37] "Renewable Energy Technologies: Cost Analysis Series - Solar Photovoltaics", International Renewable Energy Agency (IRENA), vol. 1, no. 4, Jun. 2012. [Available online: https://www.irena.org/DocumentDownloads/Publications/RE_Technologies_Cost_Analysis-SOLAR_PV.pdf (Accessed: 2017-04-10)]

[38] M. A. Green, K. Emery, Y. Hishikawa, W. Warta, E. D. Dunlop, D. H. Levi, A. W. Y. Ho-Baillie, "Solar cell efficiency tables (version 49)", *Progress in Photovoltaics*, vol. 25, no. 1, pp. 3-13, Jan. 2017.

[39] http://www.trinasolar.com/us/resources/downloads

[40] H. Moradi, A. Abtahi, R. Messenger, "Annual Performance Comparison Between Tracking and Fixed Photovoltaic Arrays", *Proceedings of the 2016 IEEE 43rd Photovoltaic Specialists Conference*, pp. 3179-3183, Jun. 2016.

[41] R. Bruno, P. Bevilacqua, L. Longo, N. Arcuri, "Small size single-axis PV trackers: control strategies and system layout for energy optimization", *70th Conference of the ATI Engineering Association*, vol. 82, pp. 737-743, Dec. 2015.

[42] http://solarpv4u.co.nz/triangle-tilt-mounting/system

[43] http://www.solar-motors.com/gb/solar-tracker-d487.shtml

[44] http://www.nrel.gov/analysis/tech_lcoe_re_cost_est.html

[45] https://www.brasit.pl/pionowa-elektrownia-wiatrowa-bof-v-5kw/

[46] https://www.rocketsolar.eu/air-30-wind-turbine.html

[47] http://www.windturbinestar.com/hawt-vs-vawt.html

[48] "Benchmarking of Small and Medium Size Wind Turbine Technologies and Legal Framework", Baltic Energy Conservation Agency (BAPE), Dec. 2013. [Available online: http://swipproject.eu/wp-content/uploads/2015/11/D1.1_2.pdf (Accessed: 2017-03-20)].

[49] http://www.motorship.com/news101/engines-and-propulsion/wartsila-installs-sofc-fuel-cell-unit-on-car-carrier

[50] "Fuel Cells", Institution of Engineering and Technology, 2009.

[51] "Transforming Power Generation and Enhancing the Resiliency of the Electric Grid", FuelCell Energy Annual Report, 2014. [Available online: http://www.annualreports.com/HostedData/AnnualReportArchive/f/NASDAQ_FCEL_2014.pdf (Accessed: 2017-03-15)]

[52] "Fuel Cells", IEA Energy Technology Essentials, 2007.

[53] https://www.capstoneturbine.com/products/c200

[54] V. A. Boicea, "Essentials of Natural Gas Microturbines", CRC Press, 2013.

[55] http://www.offgridenergy.com.au/batteries/

[56] K. C. Divya, J. Ostergaard, "Battery energy storage technology for power systems—An overview", *Electric Power System Research*, vol. 79, pp. 511-520, 2009.

[57] H. Chen, T. N. Cong, W. Yang, C. Tan, Y. Li, Y. Ding, "Progress in electrical energy storage system: A critical review" *Progress in Natural Science*, vol. 19, no. 3, pp. 291-312, Mar. 2009.

[58] F. D. González, A. Sumper, O. G. Bellmunt, R. V. Robles, "A review of energy storage technologies for wind power applications", *Renewable and Sustainable Energy Reviews*, vol. 16, pp. 2154-2171, 2012.

[59] R. Esche, "Safety of Flywheel Storage Systems", White paper Stornetic, 2016.

[60] https://gigaom.com/2011/10/31/and-the-next-solyndra-is-beacon-power/

[61] S. Schoenung, "Energy Storage System Cost Update: A Study for the DOE Energy Storage Systems Program", Sandia National Laboratories, 2011.

[62] http://www.windpowerengineering.com/design/electrical/ultracap-bank-capable-of-discharging-1-mw-for-60-sec/

[63] http://www.maxwell.com/products/ultracapacitors/modules

[64] I. Kougias, S. Szabó, F. M. Ferrario, T. Huld, K. Bódis, "A methodology for optimization of the complementarity between small-hydropower plants and solar PV systems", *Renewable Energy*, vol. 87, pp. 1023-1030, 2016.

[65] M. Surprenant, I. Hiskens, G. Venkataramanan, “Phase Locked Loop Control of Inverters in a Microgrid”, *Proceedings of the 2011 IEEE Energy Conversion Congress and Exposition*, Sep. 2011.

[66] I. Patrao, R. González-Medina, S. Marzal, G. Garcerá, E. Figueres, “Synchronization of power converters in islanded microgrids using an FM-modulated signal”, *IEEE Transactions on Smart Grid*, vol. 8, no. 1, pp. 503-510, Jan. 2017.

[67] J. Rocabert, A. Luna, F. Blaabjerg, and P. Rodriguez, “Control of Power Converters in AC Microgrids”, *IEEE Transactions on Power Electronics*, vol. 27, no. 11, pp. 4734-4739, Nov. 2012.

[68] A. Vinayagam, K. S. V. Swarna, S. Y. Khoo, A. T. Oo, A. Stojcevski, “PV Based Microgrid with Grid-Support Grid-Forming Inverter Control-(Simulation and Analysis)”, Smart Grid and Renewable Energy, vol. 8, no. 1, pp. 1-30, Jan. 2017.

[69] J. A. P. Lopes, C. L. Moreira, and A. G. Madureira, “Defining Control Strategies for Microgrids Islanded Operation”, *IEEE Transactions on Power Systems*, vol. 21, no. 2, pp. 916-924, May 2006.

[70] M. S. Mahmoud, “Microgrid: Advanced Control Methods and Renewable Energy System Integration”, 2016.

[71] G. Buigues, A. Dysko, V. Valverde, I. Zamora, E. Fernández, “Microgrid Protection: Technical challenges and existing techniques”, *International Conference on Renewable Energies And Power Quality (ICREPQ’13)*, no. 11, Mar. 2013.

[72] H. Nikkhajoei, R. H. Lasseter, “Microgrid Protection”, *Proceedings of the 2007 IEEE PES General Meeting*, pp. 1-6, Jun. 2007.

[73] ABB, “ANSI numbers”, IEEE Standard Electric Power System Device Function Numbers acc. to IEEE C.37.2-1991, Jul. 1998.

[74] N. Jenkins, X. Wu, N. Jayawarna, Y. Zhang, J. P. Lopes et al, “Protection guidelines for a microgrid”, *CORDIS*, pp. 1-370, 2005.

[75] H. Al-Nasseri, M. A. Redfern, F. Li, “A voltage based protection for micro-grids containing power electronic converters”, *Proceedings of the 2006 IEEE Power Engineering Society General Meeting*, pp. 1-7, 2006.

[76] M. Dewadasa, A. Ghosh, G. Ledwich, “Distance protection solution for a converter controlled microgrid”, *Proceedings of the 15th National Power Systems Conference*, pp. 1-661, Dec. 2008.

[77] M. Dewadasa, A. Ghosh, G. Ledwich “Protection of Microgrids Using Differential Relays”, *Proceedings of the 2011 21st Australasian Universities Power Engineering Conference*, pp. 1-6, Sep. 2011.

[78] A. A. Memon, K. Kauhaniemi, “A critical review of AC Microgrid protection issues and available solutions”, *Electric Power System Research*, vol. 129, pp. 23-31, 2015.

[79] A. R. Haron, A. Mohamed, H. Shareef, “A Review on Protection Schemes and Coordination Techniques in Microgrid System”, *Journal of Applied Sciences*, vol. 12, pp. 101-112, 2012.

[80] L. BoTong, L. YongLi, M. Tao, “Research on earthing schemes in LV microgrids”, *Proceedings of the 2011 International Conference on Advanced Power System Automation and Protection*, pp. 1003-1007, Oct. 2011.

[81] R. M. Kamel, A. Chaouachi, K. Nagasaka, “Comparison the Performances of Three Earthing Systems for Micro-Grid Protection during the Grid Connected Mode”, *Smart Grid and Renewable Energy*, vol. 2, no. 3, pp. 206-215, Aug. 2011.

[82] A. Momeneh, M. Castilla, M. M. Ghahderijani, A. Camacho, L. G. Vicuña, “Design and Control of a Small-Scale Industrial Microgrid in Islanding Mode”, *Proceedings of the 42nd Annual Conference of the IEEE Industrial Electronics Society*, pp. 72-77, Oct. 2016.

[83] T. N. Boutsika, S. A. Papathanassiou, “Short-circuit calculations in networks with distributed generation”, *Elsevier, Electric Power Systems Research*, pp. 1181-1191, 2008.

[84] ABB, “MV/LV transformer substations: theory and examples of short-circuit calculation”, QT Technical Application Papers, Feb. 2008.

[85] P. Piagi, R. H. Lasseter, "Industrial Applications of Microgrids", Power System Engineering Research Center, University of Wisconsin-Madison, 2001.

[86] T. Loix, T. Wijnhoven, G. Deconinck, "Protection of microgrids with a high penetration of inverter-coupled energy sources. Integration of Wide-Scale Renewable Resources into the Power Delivery System", *CIGRE/IEEE PES Joint Symposium,* vol. 1, no. 6, pp. 29-31, Jul. 2009.

APPENDIX

Appendix A – Table of DER technologies

Technology		Efficiency	Power	Cost ($/kW)
Photovoltaic	mono-Si	15 to 23%	up to 10 MW	2500 - 4800 (1 - 100 kW)
	poly-Si	13 to 16%		1700 - 3300 (100 - 1000 kW)
	a-Si	5 to 10%		1300 - 2700 (1 - 10 MW)
Wind turbine	HAWT	20 to 50%	up to 10 MW	4000 - 10000 (1 - 100 kW)
				2300 - 5200 (100 - 1000 kW)
	VAWT	20 to 40%		1500 - 3200 (1 - 10 MW)
Fuel cell	PEMFC	25 to 35%	up to 100 kW	1800 - 2000
	SOFC	50 to 60%	up to 300 kW	1500 - 1600
	MCFC	43 to 47%	200 kW to 3 MW	
	PAFC	40 to 42%	100 to 400 kW	4000 - 4500
Micro turbine		25 to 30%	30 kW to 1 MW	500 - 3000
Battery storage	Li-ion	75 to 90%	up to 50 MW	1200 - 4000
	Pb-A	70 to 90%	up to 20 MW	300 - 600
	Ni-based	72 to 78%	up to 50 MW	500 - 1500
Flywheel		85 to 95%	up to 20 MW	200 - 600
Supercapacitor		90 to 95%	up to 300 kW	100 - 500

Appendix B – Conference papers